67-16,515

YARGER, Douglas Neal, 1937-

THE DETERMINATION OF ATMOSPHERIC PROPERTIES BY THE MATHEMATICAL INVERSION OF THE RADIATIVE TRANSFER EQUATION.

University of Arizona, Ph.D., 1967
Physics, meteorology

University Microfilms, Inc., Ann Arbor, Michigan

THE DETERMINATION OF ATMOSPHERIC PROPERTIES BY THE MATHEMATICAL INVERSION OF THE RADIATIVE TRANSFER EQUATION

by

Douglas Neal Yarger

A Dissertation Submitted to the Faculty of the

DEPARTMENT OF METEOROLOGY

In Partial Fulfillment of the Requirements
For the Degree of

DOCTOR OF PHILOSOPHY

In the Graduate College

THE UNIVERSITY OF ARIZONA

1 9 6 7

THE UNIVERSITY OF ARIZONA

GRADUATE COLLEGE

I hereby recommend that this dissertation prepared under my direction by Douglas N. Yarger

entitled The Determination of Atmospheric Properties by the Mathematical Inversion of the Radiative Transfer Equation

be accepted as fulfilling the dissertation requirement of the degree of Doctor of Philosophy

Eugene M. Dorman — Dissertation Director — June 22, 1967 — Date

After inspection of the dissertation, the following members of the Final Examination Committee concur in its approval and recommend its acceptance:*

Stuart A. Lowitt	6/22/67
W. D. Sellers	6/22/67
A. E. Lemmon	6/25/67
Ulrich N. Bentz	6-26-67

*This approval and acceptance is contingent on the candidate's adequate performance and defense of this dissertation at the final oral examination. The inclusion of this sheet bound into the library copy of the dissertation is evidence of satisfactory performance at the final examination.

STATEMENT BY AUTHOR

This dissertation has been submitted in partial fulfillment of requirements for an advanced degree at The University of Arizona and is deposited in the University Library to be made available to borrowers under rules of the Library.

Brief quotations from this dissertation are allowable without special permission, provided that accurate acknowledgment of source is made. Requests for permission for extended quotation from or reproduction of this manuscript in whole or in part may be granted by the head of the major department or the Dean of the Graduate College when in his judgment the proposed use of the material is in the interests of scholarship. In all other instances, however, permission must be obtained from the author.

SIGNED: Douglas N Gargan

ACKNOWLEDGMENTS

I wish to express my sincere appreciation to Dr. Benjamin M. Herman for his many contributions to this dissertation. In addition to his initial suggestions for this study, his insight and continual enthusiasm in all phases of this study are gratefully acknowledged.

I also wish to thank Dr. William D. Sellers for many helpful discussions, especially in the section pertaining to the statistical study. General (ret.) S. R. Browning made several significant contributions in assisting the programming of the problem for the computer. The preliminary calculations were performed on the IBM 7072 computer at the Systems Engineering Laboratory at The University of Arizona. The final calculations were performed on the CDC 6600 computer at the NCAR facility in Boulder, Colorado. Both groups are sincerely thanked for their many special efforts.

Finally I wish to thank my wife, Sharon, for her patience and encouragement during this entire graduate program.

This work was supported by the Office of Naval Research.

TABLE OF CONTENTS

TABLE OF CONTENTS (Continued)

LIST OF FIGURES

LIST OF FIGURES (Continued)

LIST OF TABLES

ABSTRACT

A method for the determination of the vertical distribution of ozone from a satellite is discussed in this dissertation. The equation of radiative transfer is inverted using a technique originated by Phillips (1962) and further developed by Twomey (1963). The inversion is based on simulated measurements from the top of the atmosphere of the ultraviolet radiation backscattered from the earth's atmosphere. Solutions are presented only for a plane-parallel atmosphere but consider all orders of scattering and polarization.

Although the method lacks practical application at this time, the results indicate that the inversion procedure presented would provide a potentially superior method of monitoring the vertical distribution on a world-wide basis using a satellite if spherical effects could be included in the theory. A second differencing constraint is used in the inversion method, hence there is no bias toward some standard distribution.

Results where 1% random errors in the backscattered intensities are considered are compared with ozonesonde soundings, Umkehr distributions and results obtained by means of a statistical distribution. The inverse method is especially effective at levels above the ozone maximum.

Results indicate that the main maximum can be reliably found and there also are some indications of resolving certain secondary maxima. In all respects, with the limitation of the assumption of a plane-parallel atmosphere, the inverse method is at least as good as the Umkehr and statistical methods and surpasses them in many respects.

CHAPTER I

INTRODUCTION

There is a large class of physical measurement problems that falls under the general classification of indirect sensing. Here indirect sensing will be understood to have the meaning that Twomey (1965) assigned. He limited the indirect sensing problems to those where the desired function $f(x)$ is to be inferred from direct physical measurements of some other function $g(y)$ when $g(y)=\int_a^b K(x,y) f(x)dx$. The kernel function $K(x,y)$ is typically an angular scattering pattern, a spectral response, etc. It is often a smooth, monotonic function.

Frequently an investigator will make measurements of electromagnetic energy, either as a function of wavelength or angle, in order to infer characteristics of some physical parameter. This type of problem often occurs in attempts to determine various atmospheric parameters. Recently King (1966) and Wark and Fleming (1966) have published theoretical methods for the determination of atmospheric temperature profiles using radiometric measurements taken from constant level balloons. These methods appeared to give good approximations to the radiosonde soundings when actual radiometric data were used. Experiments to determine the atmospheric

water vapor content have been undertaken on the Tiros II, III and IV satellites (Bandeen 1966). Möller (1961, 1962) and Raschke (1964) have made significant theoretical contributions to this problem. The problem of determining the size and number distributions of atmospheric aerosols has attracted the attention of a large number of investigators. Newkirk and Eddy (1964) present a very complete discussion on the status of this problem up to 1963. More recently, Sekera (1966) has discussed further progress and suggested new approaches to the problem.

The problem considered in this dissertation concerns the determination of the vertical ozone distribution by the mathematical inversion of the radiative transfer equation. Ozone is of current meteorological interest for several reasons. Various workers (Schröer 1949,[1] Dutsch 1946, Craig 1948) computed the latitudinal variation of ozone based on the photochemical theory. They found a summer maximum and a winter minimum of total ozone, with a latitudinal gradient such that ozone should decrease from the poles to the equator. These photochemical predictions are in direct contradiction to observations. Because the ozone mixing ratio is a conservative property of the atmosphere below about 30 km, the explanation for the observed seasonal and latitudinal distribution must come from an understanding of

---

1. This work was actually finished in 1944.

the general circulation of the atmosphere. Consequently, any acceptable theory of the general circulation must be consistent with the observed ozone distribution.

Because of the highly absorptive character of the Hartley bands centered near 2600 Å, ozone plays a large role in the radiation balance of the stratosphere and mesosphere. It is also suspected that the effect of solar disturbances is coupled to terrestrial weather conditions through photochemical variations in ozone (Willett 1965).

In a report to the National Academy of Science by the panel on ozone (Atmospheric Ozone Studies 1965), the suggested primary focal point for extended observations and research in atmospheric ozone involves the study of its formation in the stratosphere, its transport downward into the troposphere, and its ultimate destruction at the earth's surface. It is stressed that it is important to get widespread coverage of the total ozone amounts and also vertical ozone distributions as these are important aids in the study of the properties of the general circulation of the upper troposphere and lower stratosphere.

The first published results of an inversion method to determine the vertical ozone distribution was by Götz, Meethan, and Dobson (1934). They were able to infer the main features of the vertical ozone distribution by making measurements of the Götz (1931) Umkehr effect. The Umkehr method, which is still widely used, consists essentially of

a comparison of the scattered intensities, for two different wavelengths, λ and λ', of the zenith sky light. The former is highly absorbed by ozone and the latter weakly absorbed. The ratio of the intensities at λ and λ' is measured as a function of solar elevation angle, for low elevation angles. The ozone distributions may then be computed from these measured values on the assumption of single scattering only (Ramanathan and Dave 1957). Herman and Yarger (1965) showed how all orders of scattering influence these results.

One basic problem with the Umkehr method, which was duly noted by Götz et al. (1934) in their original paper, concerns the problem of non-uniqueness. This problem has been very carefully considered by Mateer (1964), and a standard evaluation technique has been proposed (Mateer and Dutsch 1964). The Umkehr method is also ground based, which limits its usefulness in a global ozone monitoring system.

Another inversion technique that has been attempted (Epstein, Osterberg and Adel 1956, Goody and Roach 1956, and Dave, Sheppard and Walshaw 1962) concerns the determination of the vertical distribution of ozone from a series of measurements of sky emission at different air masses. The 9.6μ ozone band was used, but due to the contribution to the emission by other atmospheric constituents such as water vapor and aerosols, the results obtained were generally quite poor, and this method has essentially been abandoned.

Direct measurements were first employed by E. Regener and V. H. Regener (1934) who used an ultraviolet quartz spectrograph suspended below a balloon to measure the vertical distribution of ozone up to 32 km. Rocket-borne equipment was initiated by Johnson et al. (1952). Also, a variety of more sophisticated ozone detection instruments to be flown with balloons has been developed (Kulcke and Patezold 1957, Vassy 1958, Brewer and Milford 1960 and Regener 1960). Of the many published reports of the results of the extended ozonesonde observations, those of Hering (1962), Hering and Borden (1964-1965) and Dütsch (1966) merit special mention. The ozonesonde measurements seem to give good relative distributions, but due to calibration problems the results require normalization to the total ozone amount as determined from a Dobson spectrophotometer at some nearby ground station.

Twilight balloon (Pittock 1963) or satellite photometry (Venkateswaren, Moore and Kreuger 1961) methods involve the spectrophotometry of light which has passed tangentially through the atmosphere. By making ground based measurements at two wavelengths, λ and λ', where λ is highly absorbed and λ' weakly absorbed, it is possible to derive the total equivalent thickness of ozone in the tangential path traversed. This may then be related, by means of the geometry of the tangential path, to the vertical distribution of ozone. This method seems to be primarily sensitive to

the lower stratosphere, and also has the disadvantage of averaging over a large horizontal extent.

Observations have been made from satellites by Rawcliffe et al. (1963) and Miller and Stewart (1965). Both groups made direct solar observations, and deduced vertical distributions from the variations in attenuation of the solar beam as the path length between the satellite and sun varied. Experimental results showed fairly good agreement with rocket measurements in the region between about 40 to 80 km.

A method to determine the vertical distribution of ozone, by making spectral measurements from a satellite of the ultraviolet radiation back scattered from the earth's atmosphere, was first proposed by Singer and Wentworth (1957). They considered only primary scattering, and computed the rate at which the contribution to diffusely reflected radiation along the nadir changes as a function of optical depth in the atmosphere. Their method is applicable to regions above the ozone maximum, as is a similar method proposed by Kaplan (1961). An attempt to evaluate the effect of neglecting the contribution of radiation from the lower atmosphere to the diffusely reflected radiation emergent from the top of the atmosphere was undertaken by Sekera and Dave (1961). They concluded that scattering from all regions of the atmosphere must be considered if reliable results are to be expected. Twomey (1961) also investigated the possibility

of using spectral measurements to deduce the distribution of ozone. He investigated the influence of errors on the distribution and concluded that accurate measurements (1 per cent) could give useful information about the vertical ozone distribution down to the region around the ozone maximum (about 25 km). A later paper (Twomey and Howell 1963) discussed the limitations of direct sounding methods and showed that there can be a fundamental instability in the inversion process, which generally limits the resolving power of indirect soundings. A general approach to limit the inherent unstable nature of the inversion procedure was first suggested by Phillips (1962) and further extended by Twomey (1963, 1965). An attempt to utilize this technique was proposed by Dave and Mateer (1965). They used only primary scattering and neglected any polarization effects.

A common fault with all pre-existing methods of determining the vertical distribution of ozone from a satellite which utilize the measurements of backscattered ultraviolet radiation concerns the fact that they all neglect polarization effects and at best make approximate corrections for multiple scattering. By utilizing polarization as well as multiple scattering in the inversion equations the radiative transfer equation more nearly describes the actual physical situation. Further, one can measure two intensity components polarized at right angles to each other, instead of merely the sum of these two components (i.e. the total intensity), thus providing

twice as much information if so desired. An evaluation of this inversion method, along with a comparison with other methods for determining the vertical ozone distributions, will be presented.

CHAPTER II

FORMULATION OF THE PROBLEM

Finite Difference Formulation.

A numerical method for solving the equation of radiative transfer for a plane parallel homogeneous medium has been presented by Herman (1963) and Herman and Browning (1965). The numerical scheme utilizes a Gauss-Seidel iterative technique and has no restrictions on the form of the phase function, the occurrence of absorption, or the total optical depth. The method presented by Herman and Browning (1965) utilizes the Stokes (1852) representation for polarized light and therefore expresses the scattering phase function as a matrix. If polarization effects are ignored, the formal solution to the equation of radiative transfer becomes greatly simplified, since the scattering phase function may then be treated as a scalar.

The scalar equations representing the formal solution to the equation of radiative transfer for a plane parallel, horizontally homogeneous, absorbing atmosphere, illuminated at the top ($\tau=0$) by plane parallel radiation of $F_\nu^{(0)}$ units per unit area normal to the direction of propogation are

$$I_\nu(\tau,\mu,\phi)=\int_0^\tau J_\nu(\tau',\mu,\phi)\, e^{-\frac{(\tau-\tau')}{\mu}}\, \omega(\tau')\, \frac{d\tau'}{\mu};\quad 0\leq\mu\leq 1, \qquad (2.1)$$

and

$$I_\nu(\tau,-\mu,\phi)=\int_\tau^{\tau_T} J_\nu(\tau',-\mu,\phi)e^{-\frac{(\tau'-\tau)}{\mu}}\,\omega(\tau')\,\frac{d\tau'}{\mu};\quad 0\leq\mu\leq 1. \qquad (2.2)$$

In these expressions I_ν is the total intensity of the monochromatic radiation at the frequency ν, τ is the optical depth increasing downward[1], τ_T is the total optical depth, and ϕ is the azimuthal angle measured from some appropriately chosen x-axis. The angle between the direction of propagation of I and the z axis, which is oriented in the direction of the inward normal to the top of the atmosphere, is represented by θ ($\mu=\cos\theta$). Hence, beams traveling in the $+\mu$ direction are traveling toward the ground, and beams traveling in the $-\mu$ direction are traveling toward the top of the atmosphere. The polar and azimuthal angles of the incident plane-parallel solar flux are μ_o and ϕ_o, while $\omega(\tau)$ is the albedo for single scattering and will also be more explicitly defined later. The term $J_\nu(\tau,\mu,\phi)$ is called the source function as it denotes the contribution at any level, τ, to the beam in the direction μ,ϕ arising from scattering into this direction from beams incident from all directions, μ',ϕ'. It is given by

$$J_\nu(\tau,\mu,\phi)=\int_0^{2\pi}\int_{-1}^{1} P(\mu,\mu',\phi,\phi')I_\nu(\tau,\mu',\phi')d\mu'd\phi'$$

$$+P(\mu,\mu_o,\phi,\phi_o)F_\nu^{(0)}(\tau). \qquad (2.3)$$

The function $P(\mu,\mu_o,\phi,\phi_o)$ is the Rayleigh scattering phase function given by (Chandrasekhar 1950, p. 6) as

$$P(\cos\theta)=3/4(1+\cos^2\theta), \qquad (2.4)$$

---

1. A rigorous definition of τ will be presented later.

where θ is the angle between the incident solar beam and the scattered beam, so that

$$\cos\theta=(1-\mu^2)^{1/2}(1-\mu_o^2)^{1/2}\cos(\phi-\phi_o)+\mu\mu_o. \qquad (2.5)$$

The optical depth at the height z at the frequency ν is defined by

$$\tau(z)=\int_z^\infty K_\nu^s\,\rho(z)dz+\int_z^\infty K_\nu^a\,\rho(z)dz=\tau_\nu^s+\tau_\nu^a. \qquad (2.6)$$

Here K_ν^s and K_ν^a are the mass scattering coefficient and the mass absorption coefficient of the medium for monochromatic radiation of the frequency ν. The density of air at the height z is denoted by $\rho(z)$. The contribution to the optical depth, τ, may arise from either scattering or absorption, in which case the optical depth contributions are denoted as τ_ν^s and τ_ν^a respectively. The optical depth is considered to be zero at the top of the atmosphere and is denoted by τ_T at the bottom of the atmosphere.

Because the problem under consideration in this paper concerns the description of the vertical distribution of a trace absorbing gas (ozone) with height, the following simplifications are appropriate. The scattering coefficient will be different for ozone and air molecules due to their different indices of refraction. This difference, however, may be neglected since the ozone molecules do not appreciably contribute to the scattering optical depth, even within the ozone layer. Hence the appropriate mass scattering coefficient is closely approximated by the mass

---

1. The subscript ν will be omitted hereafter when the meaning is apparent from the context.

scattering coefficient for air only. Also, since the absorption due to ozone molecules is so much larger than the absorption due to air molecules, the latter may be neglected. With these considerations, the optical depth, τ, is commonly calculated from the following relationship:

$$\tau(z)=\int_z^\infty K^S \rho(z)dz+\int_z^\infty \alpha x(z)dz. \qquad (2.7)$$

Here K^S is the mass scattering coefficient for air and $\rho(z)$ is the density of air at the height z, α is the exponential volume absorption coefficient for 1 cm of ozone at STP and x is the ozone concentration in cm per cm at STP.

Because the vertical distribution of ozone is commonly described by data taken from an ozonagram (Godson 1962), the scattering and absorptive optical depth for a layer of thickness Δp may be conveniently described by the following relationships. Values of the ozone concentration, $\Delta\Omega$, in atm-cm at STP[1] within any increment of pressure, Δp, may be determined from the corresponding area on the ozonagram from the expression

$$x=\frac{\Delta\Omega}{\Delta p}\rho g. \qquad (2.8)$$

The scattering optical depth for a layer of thickness Δp is

$$\Delta\tau^S=K^S\frac{\Delta p}{g}, \qquad (2.9)$$

while the absorption optical depth of the same layer is given by

$$\Delta\tau^a=\alpha\Delta\Omega. \qquad (2.10)$$

---

1. A brief discussion of ozone units is given in Appendix 1.

The albedo for single scattering, $\omega(\tau)$, which represents the fraction of attenuated energy that reappears as scattered energy is given by

$$\omega=\frac{\Delta\tau^s}{\Delta\tau^s+\Delta\tau^a}=\frac{\Delta\tau^s}{\Delta\tau}\ . \tag{2.11}$$

If Eqs. (2.1) and (2.2) are expressed as a system of simultaneous equations by writing the integrals in finite difference form, they may be solved numerically by a Gauss-Seidel iterative technique (Herman 1963, Herman and Browning 1965). Using this quadrature form, Eq. (2.1) may be represented by the following system of equations.

$$I^{(2)}(\mu,\phi)=\omega(1\tfrac{1}{2})\frac{3}{16\pi}\Big\{\sum_{\Delta\mu_i'\Delta\phi_j'}(1+\cos^2\theta)\overline{I^{(1)}(\Delta\mu_i',\Delta\phi_j')}\Delta\mu_i'\Delta\phi_j' + (1+\cos^2\theta_o)F^{(0)}e^{-\frac{\Delta\tau}{2\mu_o}}\Big\}\left(1-e^{-\frac{\Delta\tau}{\mu}}\right) \tag{2.12}$$

$$I^{(3)}(\mu,\phi)=\omega(2)\frac{3}{16\pi}\Big\{\sum_{\Delta\mu_i'\Delta\phi_j'}(1+\cos^2\theta)\overline{I^{(2)}(\Delta\mu_i',\Delta\phi_j')}\Delta\mu_i'\Delta\phi_j' + (1+\cos^2\theta)F^{(0)}e^{-\frac{\Delta\tau}{\mu_o}}\Big\}\left(1-e^{-\frac{2\Delta\tau}{\mu}}\right) \tag{2.13}$$

$$\vdots$$

$$I^{(n+1)}(\mu,\phi)=I^{n-1}(\mu,\phi)e^{-\frac{2\Delta\tau}{\mu}}+\frac{3}{16\pi}\omega(n)\Big\{\sum_{\Delta\mu_i'\Delta\phi_j'}(1+\cos^2\theta)\overline{I^{(n)}(\Delta\mu_i',\Delta\phi_j')}\Delta\mu_i'\Delta\phi_j' + (1+\cos^2\theta_o)F^{(0)}e^{-\frac{n\Delta\tau}{\mu_o}}\Big\}\left(1-e^{-\frac{2\Delta\tau}{\mu}}\right) \tag{2.14}$$

where $n=3,4,5,\ldots,N-1$. Here the averages indicated above are mean values over the interval from μ_i' to μ_{i-1}' and

ϕ_j' to ϕ_{j-1}'.[1] These equations represent all of the downward traveling intensities. The upward traveling intensities may be calculated from the following finite difference form of Eq. (2.2).

$$I^{(N-1)}(-\mu,\phi)=\omega(N-1/2)\frac{3}{16\pi}\{\sum_{\Delta\mu_i'}\sum_{\Delta\phi_j'}(1+\cos^2\theta)I^{(N)}(\Delta\mu_i',\Delta\phi_j')\overline{\Delta\mu_i'\Delta\phi_j'}+(1+\cos^2\theta_o)F^{(0)}e^{-(N-1/2)\frac{\Delta\tau}{\mu_o}}\}(1-e^{-\frac{\Delta\tau}{|\mu|}}) \quad (2.15)$$

$$\vdots$$

$$I^{(N-n-1)}(-\mu,\phi)=I^{(N-n+1)}(-\mu,\phi)e^{-\frac{2\Delta\tau}{|\mu|}}+\frac{3}{16\pi}\omega(N-n)\{\sum_{\Delta\mu_i'}\sum_{\Delta\phi_j'}\overline{(1+\cos^2\theta)\times I^{(N-n)}(\Delta\mu_i',\Delta\phi_j')\Delta\mu_i'\Delta\phi_j'}+(1+\cos^2\theta_o)F^{(0)}e^{-(N-n)\frac{\Delta\tau}{\mu_o}}\}(1-e^{-\frac{2\Delta\tau}{|\mu|}}), \quad (2.16)$$

where $n=1,2,3,\ldots,N-2$.

Here N represents the total number of levels, the number of layers being N-1. Equations (2.12) through (2.16) represent M equations in M unknowns where now M is the product of the number of layers and the number of unknown intensities at each layer. The unknowns in this case are the intensities which appear on both sides of the equation. Hence, a Gauss-Seidel iteration scheme is employed. The stability and convergence criteria for the above system of equations is

---

1. Details of the assumptions involved in the averaging processes are discussed by Herman (1963) and Herman and Browning (1965).

discussed by Herman (1963) and Herman and Browning (1965). For the above system of equations the known intensities are specified by the boundary conditions at the top and bottom of the atmosphere. The incident intensities at the top of the atmosphere are considered zero while the intensities in the upward direction at the bottom of the atmosphere are constrained by the nature of the reflective properties of the ground. For the case where complete absorption at the ground surface is considered the upward intensities at the ground are also zero. All other intensities are originally unknown. The values of the single scattering albedos are specified at the midpoint of the first and last layers and at all of the intermediate levels.

The basic philosophy behind the inverse scheme is to retain the basic system of M equations and M unknowns, but to measure now N-1 intensities which allows one to solve for N-1 other unknowns; namely, the single scattering albedos. For practical considerations, the most convenient intensities to specify are those at either the top or the bottom of the atmosphere. For the remaining discussion we will assume we can specify in some manner (e.g. from measurements taken from a satellite) the intensities emergent from the top of the atmosphere. For this problem, these intensities are specified for a single wavelength as a function of angle.

The set of equations that describe these intensities emergent from the top of the atmosphere may be obtained from Eq. (2.16) by letting n=N-2.

$$I^{(1)}(-\mu,\phi)=I^{(3)}(-\mu,\phi)e^{-\frac{2\Delta\tau}{|\mu|}}+\frac{3}{16\pi}\omega(2)\{\sum_{\Delta\mu_i'}\sum_{\Delta\phi_j'}\overline{(1+\cos^2\theta)}$$

$$\overline{\times I^{(2)}(\Delta\mu_i',\Delta\phi_j')\Delta\mu_i'\Delta\phi_j'}+(1+\cos^2\theta_o)F^{(0)}e^{-\frac{2\Delta\tau}{\mu_o}}\}(1-e^{-\frac{2\Delta\tau}{|\mu|}}) \quad (2.17)$$

Physically, Eq. (2.17) states that the intensity emergent from the top of the atmosphere (i.e. level 1) in the direction $-\mu,\phi$ is equal to the intensity emergent from level 3 in the direction $-\mu,\phi$ attenuated by the optical path length, $2\Delta\tau/|\mu|$, plus the contributions to the upward intensity in the interval between level 3 and level 1 due to scattering from all other directions into the direction specified by $-\mu,\phi$. By making use of Eq. (2.16) for successively lower levels, the first term on the right hand side of Eq. (2.17) may be replaced by a summation of terms similar to the second term on the right hand side of Eq. (2.17), and results in an equation of the form

$$I^{(1)}(-\mu,\phi)=I^{(N)}(-\mu,\phi)e^{-\frac{(N-1)\Delta\tau}{|\mu|}}+\frac{3}{16\pi}\sum_{m=1}^{\frac{(N-1)}{2}}\omega(2m)\{\sum_{\Delta\mu_i'}\sum_{\Delta\phi_j'}$$

$$\overline{(1+\cos^2\theta)\times I^{(2m)}(\Delta\mu_i',\Delta\phi_j')\Delta\mu_i'\Delta\phi_j'}+(1+\cos^2\theta_o)F^{(0)}e^{-\frac{2m\Delta\tau}{\mu_o}}\}$$

$$(\exp\frac{2(m-1)\Delta\tau}{|\mu|}-\exp\frac{2m\Delta\tau}{|\mu|}). \quad (2.18)$$

The intensity, $I^{(N)}(-\mu,\phi)$, in the first term on the right hand side of Eq. (2.18) is a function of the intensities incident on the surface of the earth and the reflective properties of the surface of the earth. For simplicity the

earth's surface will be assumed to be perfectly absorbing for all wavelengths of interest, hence $I^{(N)}(-\mu,\phi)$ will be equal to zero. Also, if the single scattering albedos are expressed in terms of the midpoints of each of the layers Eq. (2.18) may be written in the following form:

$$I^{(1)}(-\mu,\phi)=\frac{3}{16\pi}\omega(1\tfrac{1}{2})\{\sum_{\Delta\mu_i'}\sum_{\Delta\phi_j'}(1+\cos^2\theta)I^{(1\frac{1}{2})}(\Delta\mu_i',\Delta\phi_j')\Delta\mu_i'\Delta\phi_j'$$

$$+(1+\cos^2\theta_o)F^{(0)}e^{-\frac{1}{2}\frac{\Delta\tau}{\mu_o}}\}\times(1-e^{-\frac{\Delta\tau}{|\mu|}})+\frac{3}{16\pi}\omega(2\tfrac{1}{2})\{\sum_{\Delta\mu_i'}\sum_{\Delta\phi_j'}(1+\cos^2\theta)$$

$$\times I^{(2\frac{1}{2})}(\Delta\mu_i',\Delta\phi_j')\Delta\mu_i'\Delta\phi_j'+(1+\cos^2\theta_o)F^{(0)}e^{-1\frac{1}{2}\frac{\Delta\tau}{\mu_o}}\}$$

$$\times(e^{-\frac{\Delta\tau}{|\mu|}}-e^{-\frac{2\Delta\tau}{|\mu|}})+\ldots+\frac{3}{16\pi}\omega(N+\tfrac{1}{2})\{\sum_{\Delta\mu_i'}\sum_{\Delta\phi_j'}(1+\cos^2\theta)$$

$$\times I^{(N+\frac{1}{2})}(\Delta\mu_i',\Delta\phi_j')\Delta\mu_i'\Delta\phi_j'+(1+\cos^2\theta_o)F^{(0)}\exp^{-(N+\frac{1}{2})\frac{\Delta\tau}{\mu_o}}\}$$

$$\times(\exp^{-\frac{(N-1)\Delta\tau}{|\mu|}}-\exp^{-\frac{N\Delta\tau}{|\mu|}}). \qquad (2.19)$$

The relationship between the single scattering albedos expressed at the midpoints of the layers and those expressed at the bottom and top of the layers is derived in Appendix 2. Note that the intensities involved in the terms on the right hand side of Eq. (2.19) are not given by the Eqs. (2.12) through (2.16), since they are now defined at midpoints of layers instead of at the top and bottom of each layer. They may be approximated by means of some suitable interpolation process using the previously calculated intensities. Hence,

the problem at this point is reduced to determining the unknown values of the single scattering albedos in Eq. (2.19) from a knowledge of the intensities at all intermediate layers. The previous statement is an oversimplification, since upon inspecting Eqs. (2.12) through (2.16) one observes that the unknowns of interest, namely the single scattering albedos, are in those equations also. The calculational procedure will be discussed in the following chapter.

Auxiliary Equation Formulation.

The main problem in solving either Eq. (2.1) or Eq. (2.19) for the ω's involves determining the values of the source functions at any level in the atmosphere. Sekera (1963) has developed a technique, involving the so-called auxiliary equation, for determining the values of these source functions by iterating on the source functions themselves. This technique has been further discussed by Dave (1964) and Dave and Walker (1966), and has the advantage that the source functions necessary to express the intensity, degree of polarization and the direction of polarization for a particular solar geometry are obtained as a function of observation angle. This facilitates the calculation of the intensities of interest by eliminating the calculation of a large number of unwanted intensities, and thereby greatly speeds the calculational process. The functions used to describe the above mentioned quantities are the four Stokes parameters.

The first two of these parameters represent the components of the intensity parallel and perpendicular to a vertical plane through the direction of interest, (μ,ϕ). Hence, in using these first two Stokes parameters one has not only considered polarization effects, but one has, in effect, obtained twice as much information at each direction of measurement.

The Simulation Problem.

Because no balloon or satellite measurements of the intensity of radiation backscattered from the earth's atmosphere exist in the wavelength region of interest ($\lambda \sim 3200$Å), these measurements were simulated. Each ozone distribution of interest was converted from an atmospheric pressure - partial pressure of ozone relationship, as represented by an ozonagram, into a single scattering albedo versus optical depth relationship. The details of these calculations are discussed in Appendix 2. The ozone distributions chosen for study were those obtained from ozonesonde soundings that corresponded to the same dates for which Umkehr distributions were presented at the same locations. The ozonesonde soundings were assumed to represent the actual ozone distribution.

The values of the intensities emerging from the top of the atmosphere can now be obtained by iterating the set of Eqs. (2.12) through (2.16), if polarization effects are

to be ignored. If the effects of polarization are to be considered, one must use either the matrix form of Eq. (2.1) or the auxiliary equation technique of Sekera (1963) to obtain the source functions, in which case emergent intensities may be calculated from Eq. (2.1).

The accuracy of both techniques for determining the emergent radiation is dependent upon the size of the optical depth increment associated with each layer of the atmosphere. Not only can one describe more detail in the ozone distribution with small optical depth increments, but also less error arises due to numerical approximations in the calculational procedure. The optical depth increments in the simulation programs were at least a factor of two smaller than the optical depth increments associated with the inversion routines.

The calculated backscattered intensities were computed for an atmosphere with the following simplifications:

1. Clouds and other aerosol layers were neglected.
2. The atmosphere of the earth was assumed to be plane parallel and horizontally homogeneous.
3. The surface of the earth was assumed to be non-reflecting in the wavelength region of interest.
4. Any emissions in the atmosphere at the wavelength of interest, either thermal or due to some atomic transitions, were assumed to be negligible.

5. The geometry of the earth and the sun, and also properties of the atmosphere, were assumed to be constant over the period of measurement.
6. The ozone distribution was assumed to have a constant mixing ratio above 10 mb due to a lack of measurements in this region.

CHAPTER III

THE NUMERICAL SOLUTION AND THE STABILITY OF THE SYSTEM

The Gauss-Seidel Scheme.

Initially, the system of equations to be solved was Eqs. (2.12) through (2.16) and Eq. (2.19) for the case where polarization is to be neglected. The following statements will similarly apply to the set of equations based on Sekera's (1963) auxiliary equation approach. If the relationship between the single scattering albedo and optical depth is known (i.e. the absorptive properties of the atmosphere are known), Herman (1963) has shown that a Gauss-Seidel procedure for the determination of the intensities, represented in Eqs. (2.12) through (2.16), converges. These equations satisfy a sufficient, but not a necessary, condition for convergence which states that convergence is assured if the coefficient of the unknown on the left hand side of the equation is at least as large as the sum of the coefficients on the right hand side. The set of equations represented by Eq. (2.19) may be rewritten to bring the unknown single scattering albedos to the left hand side of the equation. This, however, will violate the above convergence criterion. Because it is well known that many systems of equations converge even though this test fails,

it was decided to attempt to include the modified form of Eq. (2.19) in the Gauss-Seidel iterative system.

The following calculational procedure was used. Some initial typical values for the single scattering albedos were chosen to be used in determining the initial estimate of the intensities from Eqs. (2.12) through (2.16). After these calculations for the intensities at the intermediate levels were performed, the only unknown quantities in the set of equations represented by Eq. (2.19) are the ω's (i.e. the single scattering albedos). In principle one could rewrite Eq. (2.19) in a form amenable to an iterative method as previously mentioned, and thus determine the ω's, but in practice these techniques failed to converge. The lack of success with the Gauss-Seidel technique prompted a more stringent examination of the convergence requirements for this iteration method. The more rigid convergent conditions follow if one writes Eq. (2.19) as

$$(E)=(A)(\omega). \tag{3.1}$$

Here (E) is a column vector whose elements are the known intensities emergent from the top of the atmosphere at the angles of interest, (A) is a matrix whose elements are the coefficients of the ω's in Eq. (2.19) and (ω) is a column vector whose elements are the single scattering albedos at each level. Now a necessary and sufficient condition for the convergence of a Gauss-Seidel iterative procedure, where the elements of (ω) are sought, has been shown by

Sokolnikoff (1956) to be $|\lambda|_{max}$ of $(W)<1$. In this inequality (W) is a matrix defined as $-(D+B)^{-1}(F)$, where (D) has the main diagonal of (A) but is zero elsewhere, (B) has the below-diagonal elements of (A) but is zero elsewhere, and (F) has the above-diagonal elements of (A) but is zero elsewhere, and $|\lambda|_{max}$ is the absolute value of the largest eigenvalue of (W). From the cases examined, the absolute values of the largest eigenvalue were all greater than one. Therefore, a Gauss-Seidel method cannot be used and another technique must be applied.

Properties of the Coefficient Matrix.

If one examines Eq. (3.1), an obvious method for determining the values of the elements of (ω) would be to find the inverse of (A) and operate on Eq. (3.1) from the left to obtain

$$(A)^{-1}(E)=(A)^{-1}(A)(\omega)=(\omega). \qquad (3.2)$$

The Gauss-Seidel technique is a replacement technique; that is, the unknowns are determined in a sequential order where the best estimate of each unknown is used in each solution step. This is to be contrasted with the matrix inversion method now proposed, where all elements are essentially determined simultaneously. For the problem under consideration, the last rows of the matrix (A) are very nearly parallel; that is, there is a considerable degree of interdependence between the rows.

In actual practice Eq. (3.1) should be written as

$$(E)+(\varepsilon)=(A)(\omega), \tag{3.3}$$

where (ε) is an error vector that results from the introduction of quadratures and, more seriously, from observational errors. Recall that the upward emergent intensities (E) are measured at $y_i (i=1,2,\ldots,M)$ angles, the single scattering albedos, (ω), are to be found at $\tau_j (j=1,2,\ldots,N)$ layers and the elements of the matrix (A) are the source functions or quadrature coefficients $a_{ij} (i=1,2,\ldots,M; j=1,2,\ldots,N)$. Hence, Eq. (3.3) represents M linear non-homogeneous equations. If all of the $\varepsilon_i \equiv 0$, the M equations will be independent as long as the determinant of (A) does not equal zero. This follows from the basic theorems of linear systems of equations (e.g. Bôcher 1922, pp. 43-52) and can be qualitatively seen from the following reasoning. From Cramer's rule, solutions of a non-homogeneous system of linear equations exist if the determinant of coefficients (i.e. the determinant of (A)) is not equal to zero. The determinant of (A) will be zero if two or more rows differ only by a constant multiple (i.e. they are dependent). In this case, the number of equations is less than the number of unknowns and consequently, there is no unique solution. If we now allow non-zero ε_i, every non-trivial combination of the equations represented by $(A)(\omega)$ in Eq. (3.3) that is not significantly greater than the error, is equivalent to a degree of dependence. What we now need is some quantity,

which can be related to the error, to tell us under what conditions we have linear independence. The following approach is largely due to Twomey (1965).

To test for dependence we form a linear combination of the M equations represented by Eq. (3.3) by multiplying by some arbitrary normalized multiplier ξ_i (i.e. $\sum_i \xi_i^2 = 1$). Here (ξ) is a row vector. Now Eq. (3.3) becomes

$$\sum_{i=1}^{M} \xi_i E_i + \sum_{i=1}^{M} \xi_i \epsilon_i = \sum_{i=1}^{M} \sum_{j=1}^{N} \xi_i a_{ij} \omega_j . \tag{3.4}$$

Here we see that for actual independence the inequality

$$\sum_{i=1}^{M} \sum_{j=1}^{N} \xi_i a_{ij} \omega_j > \sum_{i=1}^{M} \xi_i \epsilon_i \tag{3.5}$$

must be satisfied for any normalized vector (ξ). We cannot immediately evaluate the left hand side of Eq. (3.5) since the ω_j's are the quantities to be determined. However, from *a priori* knowledge of our physical system, we can establish an upper bound on $\sum_{j=1}^{N} \omega_j$. For this particular problem the values of ω_j must necessarily satisfy the relationship $0 \leq \omega_j \leq 1$; hence, we may set N as an upper bound. We may now simplify our analysis by making use of the Schwartz inequality and the bound on $\sum_{j=1}^{N} \omega_j$ to get

$$\left| \sum_{j=1}^{N} \omega_j \sum_{i=1}^{M} \xi_i a_{ij} \right|^2 \leq \sum_{j=1}^{N} \omega_j^2 \sum_{j=1}^{N} \{ \sum_{i=1}^{M} \xi_i a_{ij} \}^2$$

$$\leq N \sum_{j=1}^{N} \{ \sum_{i=1}^{M} \xi_i a_{ij} \}^2. \qquad (3.6)$$

Under this simplification, the condition for independence expressed by Eq. (3.5) becomes

$$N \sum_{j=1}^{N} \{ \sum_{i=1}^{M} \xi_i a_{ij} \}^2 >> \{ \sum_{i=1}^{M} \xi_i \epsilon_i \}^2. \qquad (3.7)$$

The inequality has been strengthened to compensate for the relaxed conditions that result from using the Schwartz inequality. The expression

$N \sum_{j=1}^{N} \{ \sum_{i=1}^{M} \xi_i a_{ij} \}^2$ may be written in matrix form as

$$N(\xi A)(\xi A)^* = N(\xi)(A)(A)^*(\xi)^*, \qquad (3.8)$$

where the * represents the transpose of the matrix. The matrix $(A)(A)^*$ is a real symmetric matrix and therefore has real eigenvalues, hence it would be convenient to relate the condition for independence to these eigenvalues. The smallest value of the quadratic form $(\xi)(A)(A)^*(\xi)^*$ can be related to the eigenvalues of $(A)(A)^*$ in the following manner. Let us define the matrix (U) as the matrix whose columns are the normalized eigenvectors of the matrix $(A)(A)^*$. That is,

$$(A)(A)^*(U)=(U)(\Lambda), \tag{3.9}$$

where (Λ) is a diagonal matrix whose diagonal elements are the eigenvalues. The arbitrary row vector (ξ) may be related to the matrix (U) through its transpose by the relationship

$$(\xi)^*=(U)(\eta), \tag{3.10}$$

where (η) is the column vector which satisfies Eq. (3.10) and will be more explicitly defined later.

Because the eigenvectors of the matrix $(A)(A)^*$ are orthonormal,

$$(U)^*(U)=(I), \tag{3.11}$$

where (I) is the identity matrix, it then follows from Eq. (3.9) that

$$(A)(A)^*=(U)^{*-1}(\Lambda)(U)^{-1}. \tag{3.12}$$

Now Eq. (3.8) may be transformed as follows:

$$\begin{aligned} N(\xi)(A)(A)^*(\xi)^* &= N(\eta)^*(U)^*(A)(A)^*(U)(\eta) \\ &= N(\eta)^*(U)^*(U)^{*-1}(\Lambda)(U)^{-1}(U)(\eta) \\ &= N(\eta)^*(\Lambda)(\eta) \\ &= N\sum_i \lambda_{ii}\eta_i^2 \end{aligned} \tag{3.13}$$

But $(\xi)(\xi)^*=1$, therefore,

$$(\xi)(\xi)^*=(\eta)^*(U)^*(U)(\eta)=(\eta)^*(\eta)=1. \tag{3.14}$$

Now the condition for independence of the equations expressed by Eq. (3.3) is, using Eqs. (3.7) and (3.13),

$$N \sum_{i=1}^{M} \lambda_{ii} \eta_i^2 >> \{ \sum_{i=1}^{M} \xi_i \varepsilon_i \}^2 . \qquad (3.15)$$

But $$\sum_{i=1}^{M} \{\xi_i \varepsilon_i\}^2 = (\xi\varepsilon)^*(\xi\varepsilon) = (\varepsilon)^*(\xi)^*(\xi)(\varepsilon) = (\varepsilon)^*(\varepsilon), \qquad (3.16)$$

and since an absolute minimum value of the expression $N \sum_{i=1}^{M} \lambda_{ii} \eta_i^2$ will occur when all the elements of (η) equal zero except the element $\eta_j (=1)$ corresponding to the smallest eigenvalue, λ_{jj}, it follows that the condition for true independence of the equations represented by Eq. (3.3) may be written as

$$\lambda_{ii} >> \frac{\sum_{i=1}^{M} \varepsilon_i^2}{N} . \qquad (3.17)$$

Now the dimension of independence must be reduced by one for each eigenvalue of the matrix $(A)(A)^*$ which is too small to satisfy this inequality.

CHAPTER IV

TWOMEY'S INVERSION TECHNIQUE

Preliminary Remarks.

The numerical problems in the solution of Eq. (3.3) are discussed and illustrated by Phillips (1962) and also by Twomey and Howell (1963). A characteristic feature of the numerical solutions of equations of the type illustrated by Eq. (3.3) is the large oscillations which dominate the solution. Phillips (1962) first attempted to use *a priori* physical knowledge of the solution vector (e.g. that it is a reasonably smooth function) to introduce constraints into the numerical solution. Twomey (1965) extended these techniques to include non-square coefficient matrices (i.e. the number of observations exceeds the number of unknowns) and also a variety of constraint conditions, in addition to reducing the number of required matrix inversions from two to one. In the following section the general Twomey method will be presented and applied to the inversion of Eq. (3.3).

General Formulation.

The constraints mentioned above, applied to the problem at hand, have the nature of smoothing conditions. Certain *a priori* knowledge of the physical system is assumed;

that is, it is assumed that reasonable estimates of the existing errors in the system may be found and also it is assumed that the solution will be some type of smooth function. Because the errors can be estimated, one can calculate

$$(\varepsilon)^*(\varepsilon)=\sum_i \varepsilon_i^2 = \text{constant} \tag{4.1}$$

and thus determine the value of the constant. Now the elements of (ω) are chosen such that the square of the second derivative about each solution point (evaluated numerically) is a minimum, while the condition of Eq. (4.1) is maintained. The square of the second derivative about the ith point will have the general form $(\omega_{i-1}-2\omega_i+\omega_{i+1})^2$ when the derivative is numerically evaluated. For convenience, the value of the above square at each point will be denoted as an element of the vector (Q). In order to minimize (Q), subject to the constraint of Eq. (4.1), the method devised by Lagrange (i.e. the method of undetermined multipliers) may be employed as was shown by Twomey (1965). This general technique is explained elsewhere (e.g. Margenau and Murphy 1956, Wangsness 1963) and will not be repeated here. Utilizing this technique, the solution vector (ω) may be determined from the following system of linear equations:

$$\frac{\partial}{\partial \omega_k}\{(\varepsilon)^*(\varepsilon)+\gamma(Q)\}=0, \quad k=1,2,\ldots,N, \tag{4.2}$$

where γ is the Lagrange multiplier.

In principle, it is determined from Eq. (4.2), once the upper bound on the errors is determined, as that multiplier which results in the proper value of $\sum_i \varepsilon_i^2$. For any γ, the resulting errors associated with the solution vector are determined by calculating values of the reflected intensities from Eq. (3.1). The errors may then be found by comparing the resulting values of the reflected intensities with the known values. For the proper choice of Lagrange multiplier, the sum of the squares of these errors should approximately equal the *a priori* estimated errors. Because the solution is a slowly varying function of the Lagrange multiplier, the selection of a proper value for this multiplier within a factor of ten is usually sufficient. The actual numerical considerations are discussed in more detail in the following chapter.

Eq. (4.2) will now be more explicitly evaluated in the discussion which follows. The first term of Eq. (4.2), $\frac{\partial}{\partial \omega_k} (\varepsilon)^*(\varepsilon)$, may be rewritten using Eq. (3.3) as

$$\frac{\partial}{\partial \omega_k}((A)(\omega)-(E))^*((A)(\omega)-(E)).$$

Since the operation $\frac{\partial}{\partial \omega_k} (\omega)$ gives a column vector with zeros in all but the kth element, define $\frac{\partial}{\partial \omega_k} \equiv (d_k)$ and $\frac{\partial}{\partial \omega_k} (\omega)^* \equiv (d_k)^*$. Now the expression to be evaluated is

$$\frac{\partial}{\partial \omega_k}((A)(\omega)-(E))^*((A)(\omega)-(E))$$

$$= \frac{\partial}{\partial \omega_k}((\omega)^*(A)^*-(E)^*)((A)(\omega)-(E))$$

$$= \frac{\partial}{\partial \omega_k}((\omega)^*(A)^*(A)(\omega)-(E)^*(A)(\omega)-(\omega)^*(A)^*(E)+(E)^*(E)) \tag{4.3}$$

$$=(d_k)^*(A)^*(A)(\omega)+(\omega)^*(A)^*(A)(d_k)-(E)^*(A)(d_k)-(d_k)^*(A)^*(E),$$

where k=1,2,...,N. The first term on the right hand side of Eq. (4.3) is equal to the transpose of the second term and the third term is equal to the transpose of the fourth term. Therefore, since each term on the right hand side of Eq. (4.3) is a scalar, the first and second terms are equal and the third and fourth terms are equal, and we may write

$$\frac{\partial}{\partial \omega_k}(\varepsilon)^*(\varepsilon)=2(d_k)^*(A)^*(A)(\omega)-2(d_k)^*(A)^*(E), \tag{4.4}$$

where k=1,2,...,N. Premultiplying a matrix by $(d_k)^*$ amounts to extracting the kth row of the matrix, hence the above system of equations may be written as a single matrix expression as $2(A)^*(A)(\omega)-2(A)^*(E)$.

A Discussion of the Matrix (Q).

The second term in Eq. (4.2) remains to be evaluated. However, because the exact form of the matrix (Q) is somewhat arbitrary due to various possible descriptions of the physical characteristics at the top and bottom of the

atmosphere, several examples will be considered. Since the numerical evaluation of a second difference requires a knowledge of the values of the function at three points, some decision must be made concerning the evaluation of the second derivative in the region of the top and bottom boundary. Twomey (1965) makes no assumptions about the boundary and chooses to begin the second differencing constraint at the second interior data point. To evaluate $\frac{\partial}{\partial \omega_k}$ (Q) obtained with this assumption, let us consider a solution vector consisting of five evenly spaced data points, ω_k, $k=1,2,\ldots,5$. Twomey's assumptions would require the following numerical form of the second derivative with respect to each of the ω_k:

$$\sum_{i=2}^{4} (\omega_{i-1} - 2\omega_i + \omega_{i+1})^2 = \{(\omega_1 - 2\omega_2 + \omega_3)^2 + (\omega_2 - 2\omega_3 - \omega_4)^2 + (\omega_3 - 2\omega_4 - \omega_5)^2\}. \tag{4.5}$$

The results of operating on Eq. (4.5) with each of the five partial derivatives with respect to ω_k gives

$$\frac{\partial}{\partial \omega_1}\{\ \} = 2(\omega_1 - 2\omega_2 + \omega_3), \tag{4.6}$$

$$\frac{\partial}{\partial \omega_2}\{\ \} = 2(-2\omega_1 + 5\omega_2 - 4\omega_3 + \omega_4), \tag{4.7}$$

$$\frac{\partial}{\partial \omega_3}\{\ \} = 2(\omega_1 - 4\omega_2 + 6\omega_3 - 4\omega_4 + \omega_5), \tag{4.8}$$

$$\frac{\partial}{\partial \omega_4}\{\ \} = 2(\omega_2 - 4\omega_3 + 5\omega_4 - 2\omega_5), \tag{4.9}$$

$$\frac{\partial}{\partial \omega_5}\{\ \} = 2(\omega_3 - 2\omega_4 + \omega_5). \tag{4.10}$$

The right hand sides of the above equations may be written as a single matrix expression as $2(H)(\omega)$, where the matrix (H) has the following form:

$$\begin{vmatrix} 1 & -2 & 1 & 0 & 0 \\ -2 & 5 & -4 & 1 & 0 \\ 1 & -4 & 6 & -4 & 1 \\ 0 & 1 & -4 & 5 & -2 \\ 0 & 0 & 1 & -2 & 1 \end{vmatrix} .$$

Now it follows that the evaluation of Eq. (4.2) leads to the matrix expression

$$(A)^*(A)(\omega) - (A)^*(E) + \gamma(H)(\omega) = 0, \tag{4.11}$$

where a constant multiple of two has been factored from the equation. The above expression has been derived for a particular form of the matrix (Q). However, Twomey (1965) shows that Eq. (4.11) has the same form for a variety of different constraints (e.g. the square of the departures of each point from a standard solution, the square of the third differences about each point, etc.) providing the proper form of the matrix (H) is derived. An important point to note in the previous example is that no constraints are placed on the first and last points. In most problems

this presents no difficulty at the top of the atmosphere where the reflected intensities contain a relatively large amount of information about the single scattering albedos, but the solution points at the bottom of the atmosphere will tend to wander due to the lack of information content in the intensities and no constraints at the boundaries.

Fleming and Wark (1965) make use of the physical knowledge of their particular problem and require that the virtual solution points outside of the boundary are zero. This influences the first and last solution points such that their values will tend to curve toward zero at the ends.

To derive the matrix (H) obtained under these assumptions five solution points will again be used. In addition the virtual solution points ω_0 and ω_6 outside of the atmosphere will be introduced with the requirement that both of these values be zero. Hence, the quantity to be minimized is the following sum with respect to ω_k, k=1,2,...,5.

$$\sum_{i=1}^{5} (\omega_{i-1}-2\omega_i+\omega_{i+1})^2=(\omega_0-2\omega_1+\omega_2)^2+(\omega_1-2\omega_2+\omega_3)^2$$

$$+(\omega_2-2\omega_3+\omega_4)^2+(\omega_3-2\omega_4+\omega_5)^2+(\omega_4-2\omega_5+\omega_6)^2 \qquad (4.12)$$

Performing operations analogous to those indicated in Eqs. (4.6) through (4.10) while noting that $\omega_0=\omega_6=0$, one obtains the following form for the matrix (H):

$$\begin{vmatrix} 5 & -4 & 1 & 0 & 0 \\ -4 & 6 & -4 & 1 & 0 \\ 1 & -4 & 6 & -4 & 1 \\ 0 & 1 & -4 & 6 & -4 \\ 0 & 0 & 1 & -4 & 5 \end{vmatrix} .$$

For the problem of determining the vertical ozone distribution, a physically more plausible condition would be to assume a constant mixing ratio of ozone at the top and bottom of the atmosphere. This is equivalent to assuming that the virtual points outside of the boundary in the present example are equal to the boundary points. This assumption has theoretical justification on the basis of photochemical theory as well as observational evidence. With the above conditions $\omega_{-1}=\omega_0=\omega_1$ and $\omega_5=\omega_6=\omega_7$, and the form of the matrix (Q) is

$$\sum_{i=0}^{6}(\omega_{i-1}-2\omega_i+\omega_{i+1})^2=(\omega_{-1}-2\omega_0+\omega_1)^2+(\omega_0-2\omega_1+\omega_2)^2$$

$$+(\omega_1-2\omega_2+\omega_3)^2+(\omega_2-2\omega_3+\omega_4)^2+(\omega_3-2\omega_4+\omega_5)^2$$

$$+(\omega_4-2\omega_5+\omega_6)^2+(\omega_5-2\omega_6+\omega_7)^2. \qquad (4.13)$$

Performing the usual differentiation with respect to ω_k, $k=1,2,\ldots,5$, one obtains the following form for the matrix (H):

$$\begin{vmatrix} 3 & -4 & 1 & 0 & 0 \\ -3 & 6 & -4 & 1 & 0 \\ 1 & -4 & 6 & -4 & 1 \\ 0 & 1 & -4 & 6 & -3 \\ 0 & 0 & 1 & -4 & 3 \end{vmatrix} .$$

Because the amount of information about the ozone distribution that is contained in the reflected intensities decreases very rapidly as one seeks information from progressively greater depths below the ozone maximum, another possible boundary condition at the ground would be to require the single scattering albedos in the lower layers to approach previously estimated typical values. Frequently one has a means of estimating typical values of the partial pressure of ozone at the surface. These ozone partial pressures may be converted into single scattering albedos in the following manner. Using Eqs. (2.9) and (2.10) it follows that

$$\Delta\tau = \alpha\Delta\Omega + \frac{K^S}{g}\Delta p, \qquad (4.14)$$

where $\Delta\tau$ is a predetermined constant optical depth increment. Godson (1962) shows that one may relate the increment of integrated ozone between two pressure levels to the average partial pressure of ozone within that level by the relationship

$$\Delta\Omega(\text{m atm-cm}) = \frac{\bar{p}_3(\mu\text{mb})\log_{10}(\frac{p_2}{p_1})}{0.55}, \qquad (4.15)$$

where $\bar{p}_3$ is the average partial pressure of ozone in the layer $\Delta p = p_2 - p_1$. Using the above expression Eq. (4.14) may now be written in terms of pressure.

$$\Delta\tau = \frac{\alpha\bar{p}_3\log_{10}(\frac{p_2}{p_1})}{0.55} + \frac{K^s}{g}(p_2 - p_1). \qquad (4.16)$$

To determine the value of the single scattering albedo that applies to the optical depth increment immediately above the surface, let p_2 be the surface pressure and p_1 the pressure, to be determined, which satisfies Eq. (4.16). After evaluating p_1 from Eq. (4.16) one can determine the single scattering albedo from

$$\omega = \frac{\frac{K^s}{g}(p_2 - p_1)}{\Delta\tau}. \qquad (4.17)$$

The equation analogous to Eq. (4.11) may be derived using the proper form of the matrix (H), which minimizes the square of the second differences about each point, with the boundary conditions of a constant mixing ratio for the virtual points outside of the atmosphere at the top and "known" single scattering albedos for the virtual points outside of the atmosphere below the surface. It now

becomes convenient to make use of Eq. (3.3) to write Eq. (4.11) as

$$(A)^*(\varepsilon)+\gamma(H)(\omega)=0. \tag{4.18}$$

Using a five layer problem as an example, Eq. (4.18) may be written more explicitly in the following terms.

$$a^*_{1,1}\varepsilon_1+a^*_{1,2}\varepsilon_2+\ldots+a^*_{1,5}\varepsilon_5+\gamma h_{1,1}\omega_1+\gamma h_{1,2}\omega_2+\ldots$$

$$+\gamma h_{1,5}\omega_5+\gamma h_{1,6}\omega_6+\gamma h_{1,7}\omega_7=0$$

$$\vdots$$

$$a^*_{5,1}\varepsilon_1+a^*_{5,2}\varepsilon_2+\ldots+a^*_{5,5}\varepsilon_5+\gamma h_{5,1}\omega_1+\gamma h_{5,2}\omega_2+\ldots$$

$$+\gamma h_{5,5}\omega_5+\gamma h_{5,6}\omega_6+\gamma h_{5,7}\omega_7=0.$$

Here the first five ω's are unknown and are to be determined, while ω_6 and ω_7 are equal and are "known" constants. The general form of the matrix (H) may easily be inferred by making use of the form that follows from Eq. (4.13). The new matrix (H) will now be non-square in order to make use of the "known" virtual ω's at the bottom and has the following elements:

$$\begin{vmatrix} 3 & -4 & 1 & 0 & 0 & 0 & 0 \\ -3 & 6 & -4 & 1 & 0 & 0 & 0 \\ 1 & -4 & 6 & -4 & 1 & 0 & 0 \\ 0 & 1 & -4 & 6 & -4 & 1 & 0 \\ 0 & 0 & 1 & -4 & 6 & -4 & 1 \end{vmatrix}.$$

The elements in the upper left portion of the above matrix corresponds to the constant mixing ratio assumption at the top of the atmosphere. The set of equations (4.18) may now be written as

$$(A)*(\varepsilon)+\gamma(H)(\omega)+\gamma(H')(\omega')=0, \tag{4.19}$$

where the matrix (H) is

$$\begin{vmatrix} 3 & -4 & 1 & 0 & 0 \\ -3 & 6 & -4 & 1 & 0 \\ 1 & -4 & 6 & -4 & 1 \\ 0 & 1 & -4 & 6 & -4 \\ 0 & 0 & 1 & -4 & 6 \end{vmatrix}$$

and the matrix (H') is

$$\begin{vmatrix} 0 & 0 & 0 & 0 & 0 & 0 & 0 \\ 0 & 0 & 0 & 0 & 0 & 0 & 0 \\ 0 & 0 & 0 & 0 & 0 & 0 & 0 \\ 0 & 0 & 0 & 0 & 0 & 1 & 0 \\ 0 & 0 & 0 & 0 & 0 & -4 & 1 \end{vmatrix}.$$

The solution vector (ω) contains the five elements ω_k, $k=1,2,\ldots,5$, while the vector (ω') has zeros for the first five elements, $\omega_6' = \omega_6$ and $\omega_7' = \omega_7$; ω_6 and ω_7 being previously specified. Now we may use Eq. (3.3) again to replace (ε) in Eq. (4.19) to get

$$(A)*((A)(\omega)-(E))+\gamma(H)(\omega)+\gamma(H')(\omega')=0, \tag{4.20}$$

which may be written as

$$((A)*(A)+\gamma(H))^{-1}((A)*(E)-\gamma(H')(\omega'))=(\omega). \tag{4.21}$$

It is this equation which is used to determine the ozone distributions that will be discussed in the following chapter.

CHAPTER V

INVERSION RESULTS

Preliminary Remarks.

The selection of the ozonesonde soundings to be used in the following inversion studies was based upon several criteria. Because the technique of inverting the radiative transfer equation is to be compared with other methods of determining the ozone distribution, ozonesonde data were selected from a two year sampling program directed by Dütsch (1966). Dütsch (1966) presents measurements, made with balloon-borne Brewer-Mast electro-chemical sondes, of the vertical ozone distribution over Boulder, Colorado, for a two year period beginning in August 1963. During this same period of time Umkehr observations were also carried out at Boulder, Colorado. The results of these studies have been published by Dütsch and Mateer (1964). Ozonesonde soundings were selected which corresponded to the most reliable available Umkehr data for the corresponding time period. Because of a limited amount of available computer time, the final number of distributions to be studied was reduced to six. These six were selected because they represented quite different, but typical, distributions.

Table 5.1.

Nadir angles for which there were simulated intensity measurements.

Here $\mu=\cos\theta$ where θ is the angle from the nadir.

μ	θ	μ	θ
0.01	89°25'	0.49	60°40'
0.03	88°17'	0.55	56°38'
0.06	86°34'	0.61	52°25'
0.10	84°16'	0.67	47°56'
0.14	81°57'	0.74	42°16'
0.19	79°3'	0.82	34°55'
0.25	75°31'	0.89	27°8'
0.31	71°56'	0.94	19°57'
0.37	68°17'	0.97	14°4'
0.43	64°32'	0.99	8°6'

Calculational Considerations.

In the inversion routine the surface pressure and the total amount of ozone will be assumed independently known. Methods for determining the total amount of ozone from a satellite have been suggested by Singer and Wentworth (1957) and Dave and Mateer (1967). Although the progress is encouraging, this is still an area which requires further study. The surface pressure will be assumed determinable to within a very few percent from existing surface data. Therefore, for the present inversion study, the total optical depth ($\tau = \alpha\Omega_{total} + \frac{K^s}{g} p_{surface}$) will be assumed known for each problem.

The reflected intensities at the top of the atmosphere were calculated from the auxiliary equation using the actual single scattering albedos, as determined by the ozonesonde, at equal optical depth increments. Since the total optical depth was about 0.78 for each of the six test cases, and it was desired to use optical depth increments of about $\Delta\tau = 0.01$, the atmosphere was divided into 78 equal increments of optical depth. This resulted in optical depth increments ranging from 0.0098 to 0.0103.

The angles selected for the simulated measurement of the reflected intensities are listed in Table 5.1. The azimuthal angles were limited to $\phi = 0$ and 180 degrees, while the cosine of the nadir angle, μ, varied from 0.01 to 0.99 in unequal increments. There were sixty values of

the reflected intensities computed for the present study. These were comprised of both the I_1 and I_2 components (i.e. the first two Stokes parameters) of the total intensity (see Herman and Browning 1965) for ϕ=0 degrees and the I_1 component for ϕ=180 degrees for each value of μ. The I_2 component for ϕ=180 degrees is equal to the I_2 component for 0 degrees, hence only one of these values was used.

Very briefly, the general calculational scheme consists of the following major elements. To begin the iteration cycle, source functions were calculated using the auxiliary equation technique, for small, equally spaced optical depth increments ($\Delta\tau$=0.01) using initial estimates of the single scattering albedos corresponding to these layers. For numerical reasons (Herman and Browning 1965, p. 560) the source functions are obtained at much smaller optical depth increments than can be practically resolved in the inversion process. Therefore, for the inversion part of the routine, the number of source functions, which make up the elements of the matrix (A), are reduced by averaging over larger layers in a manner which is discussed later. These source functions that are obtained as a result of the averaging process are then used with the sixty values of the reflected intensities. The inversion process, described by Eq. (4.21), is then used to obtain new estimates of the single scattering albedos. These single scattering albedos now apply to the large layers used in the previous

Figure 5.1. An ozone distribution in terms of single scattering albedos for Feb. 8, 1964.

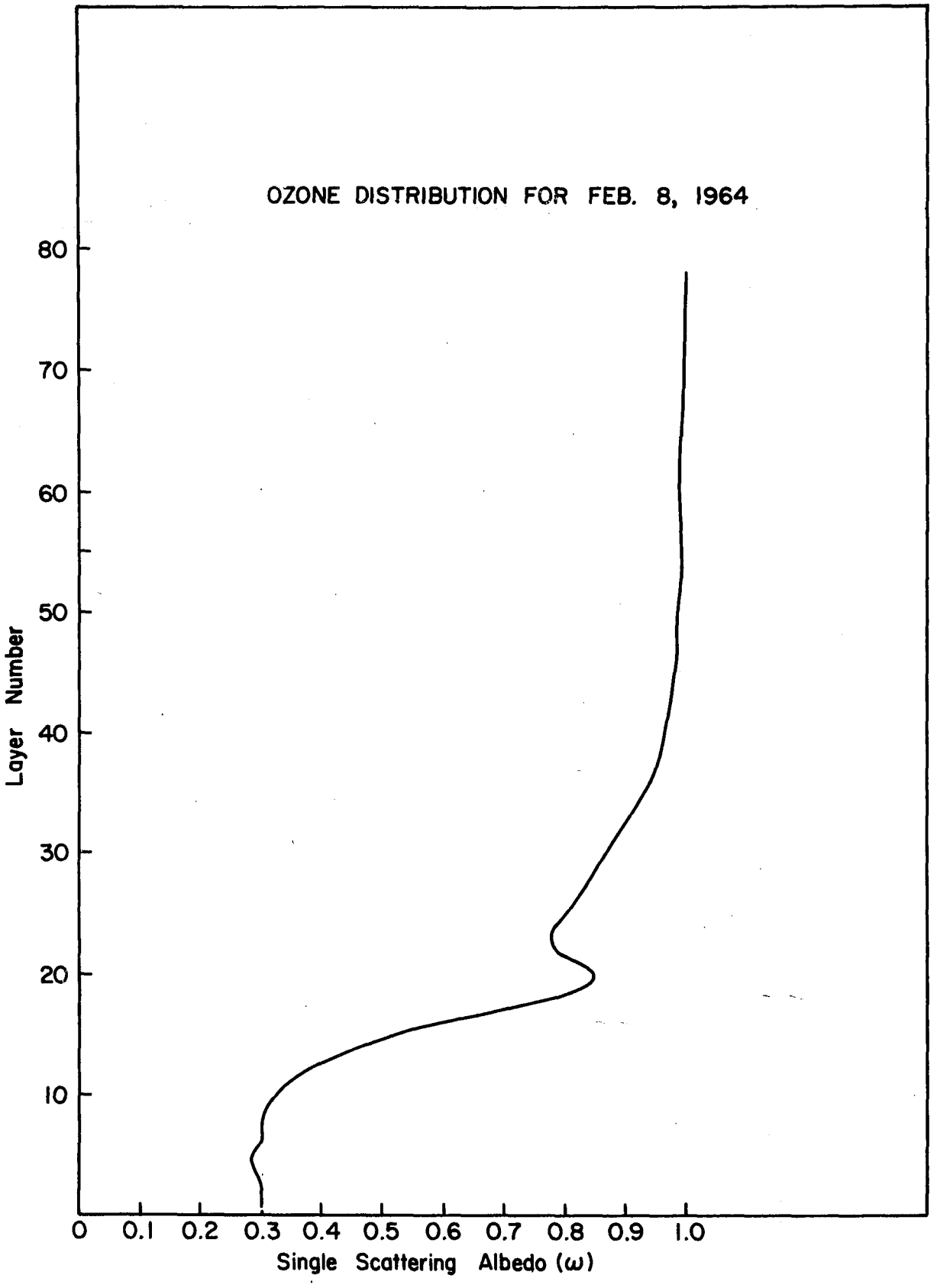
OZONE DISTRIBUTION FOR FEB. 8, 1964
Layer Number
80
70
60
50
40
30
20
10
0
0.1
0.2
0.3
0.4
0.5
0.6
0.7
0.8
0.9
1.0
Single Scattering Albedo (ω)

Figure 5.1

averaging process. Therefore, in order to begin a new iteration cycle single scattering albedos that apply to the small equal optical depth intervals are needed. These single scattering albedos are obtained by a suitable interpolation process. At this point a new iteration cycle may be begun.

Because there is inherently more information concerning the vertical distribution of ozone in the upper part of the atmosphere contained in the reflected intensities, and because the ozone distribution varies more rapidly with optical depth in the upper part of the atmosphere, the source functions correspond to averages over smaller optical depth increments at the top of the atmosphere than at the bottom. This may be seen in Fig. 5.1 which presents ozonesonde data in terms of single scattering albedos for Feb. 8, 1964.[1] If we let the basic unit of optical depth be one of the 78 equal optical depth increments used to calculate the reflected intensities ($\Delta\tau=0.01$), then the source functions were averages which apply to the following layer groups. Each of the first fifteen source functions used in the inversion were averages over two optical depth units. The sixteenth and seventeenth source function each applied to ten optical depth units, while the eighteenth and nineteenth source functions each pertained to fourteen optical depth units.

---

1. Layer one is at the top of the atmosphere and layer 78 is at the bottom.

Using the inversion technique indicated by Eq. (4.21), nineteen single scattering albedos were obtained which describe the ozone amounts in the nineteen optical depth groups previously discussed. A Newton interpolation scheme (Hamming, 1962) was then applied to these nineteen unequally spaced points to obtain 39 equally spaced single scattering albedos. By means of the relationships described in Appendix 2, these single scattering albedos were converted to a pressure versus partial pressure of ozone representation. This new ozone distribution was then converted back to 78 single scattering albedos corresponding to 78 equal optical depth increments ($\Delta\tau=0.01$). Now new source functions could be computed from the auxiliary equation using these single scattering albedos to begin a new iteration. The iteration cycle was continued until the maximum change in any single scattering albedo was less than 0.006 units. This corresponds to about a 2% change for the small single scattering albedos and about a 0.6% variation for the largest values.

Numerical Experimentation.

Several different forms of the matrix (Q) were discussed in Chapter IV. A test ten layer problem was used in order to evaluate the effects of various boundary conditions on the solution matrix. If the form of the matrix (H) is used which leaves the points outside of the atmosphere unspecified, the solution shown in Fig. 5.2

Figure 5.2. Inversion results for a ten layer test problem where the boundary conditions left the points outside of the atmosphere unspecified.

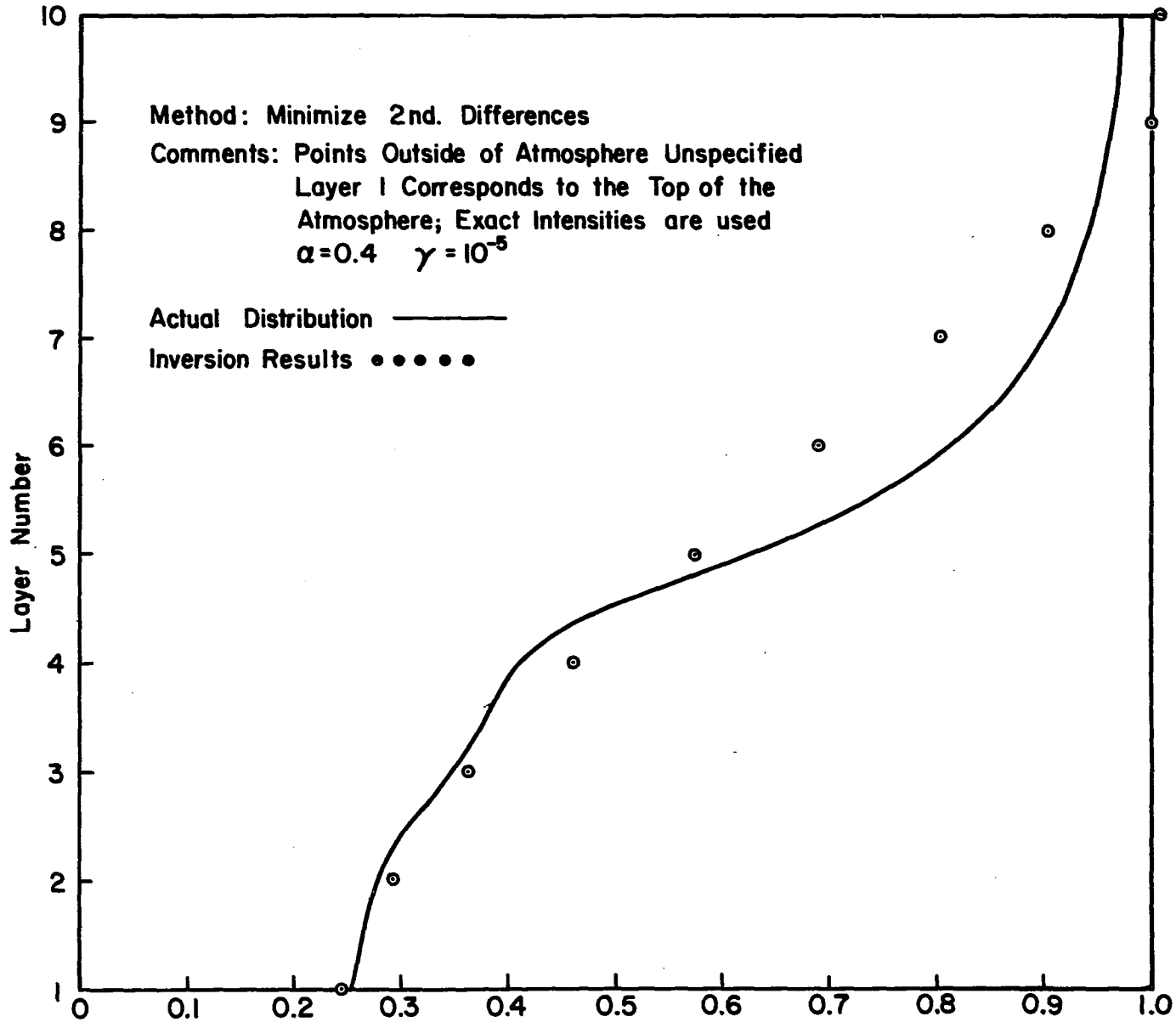
Method: Minimize 2nd. Differences
Comments: Points Outside of Atmosphere Unspecified
Layer 1 Corresponds to the Top of the
Atmosphere; Exact Intensities are used
α=0.4 γ = 10^-5
Actual Distribution
Inversion Results
Layer Number
ω
0
0.1
0.2
0.3
0.4
0.5
0.6
0.7
0.8
0.9
1.0
1
2
3
4
5
6
7
8
9
10

Figure 5.2

Figure 5.3. Inversion results for a ten layer test problem where the boundary conditions specified the points outside of the atmosphere as zero.

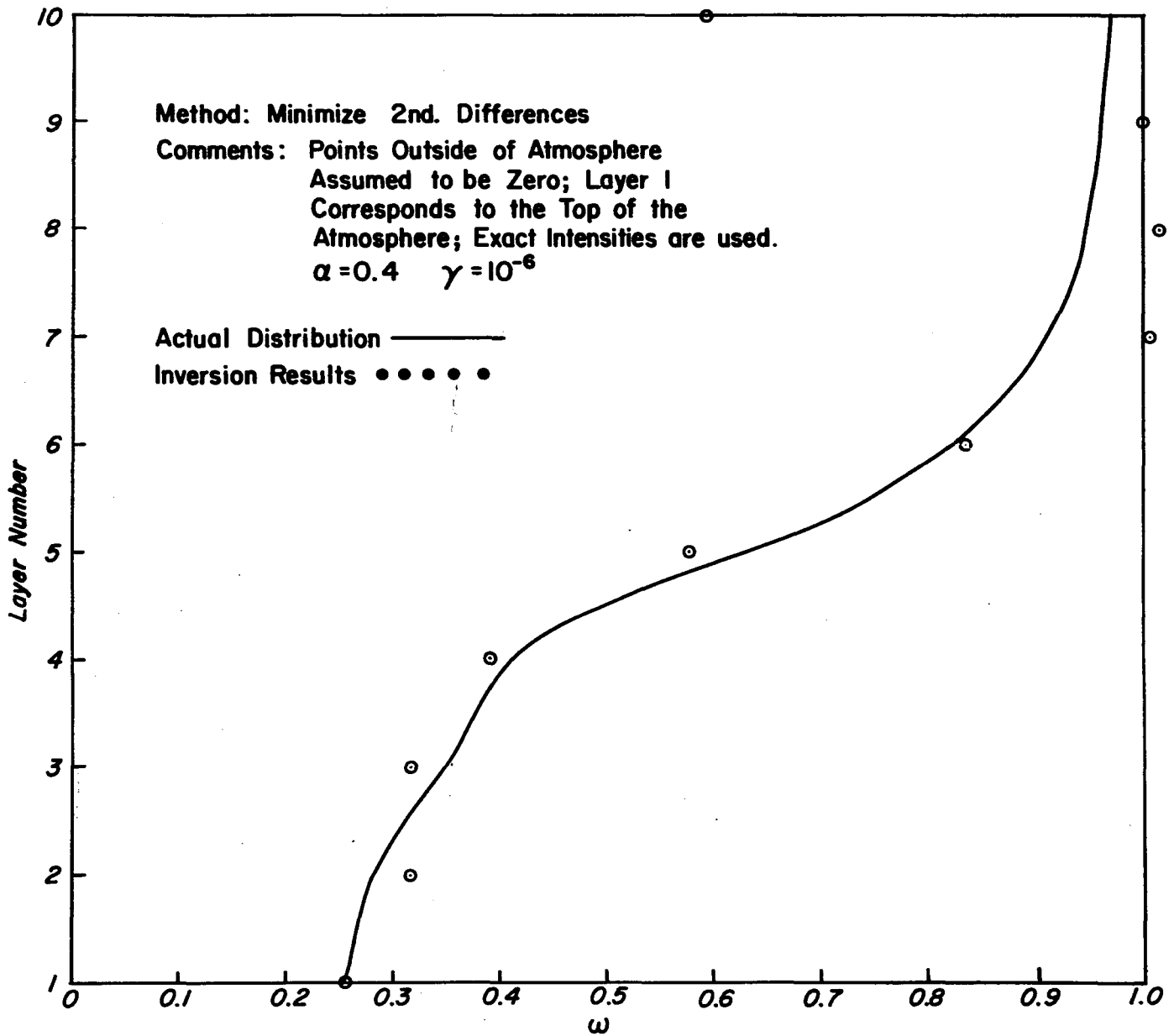
Method: Minimize 2nd. Differences
Comments: Points Outside of Atmosphere Assumed to be Zero; Layer 1 Corresponds to the Top of the Atmosphere; Exact Intensities are used.
α = 0.4 γ = 10^-6
Actual Distribution
Inversion Results
Layer Number
ω
10
9
8
7
6
5
4
3
2
1
0
0.1
0.2
0.3
0.4
0.5
0.6
0.7
0.8
0.9
1.0

Figure 5.3

is obtained. The absorption coefficient used in this solution corresponds to a wavelength near 3250Å. Also, exact values of the reflected intensities were used. Notice that the solution points (the circled points) near the top of the atmosphere agree closely with the actual values (the solid line) while the solution points in the other portions of the curve lie approximately on a straight line. The point at the bottom of the atmosphere is physically unrealistic as it exceeds unity.

If the boundary conditions used by Fleming and Wark (1965) in their particular problem (i.e. the points outside of the atmosphere are assumed zero) are used to specify the form of the matrix (H), the solution shown in Fig. 5.3 results. Again exact values of the reflected intensities were used. A very noticeable curvature of the solution points (i.e. the circled points) toward zero at both the bottom and top of the atmosphere is demonstrated. This becomes very extreme at the bottom of the atmosphere where the nature of the constraint dominates the solution. Therefore, it must be concluded that this is a poor choice of boundary conditions for this problem.

Further numerical experimentation with the boundary conditions, but using an actual ozone distribution, were performed on the large CDC 6600 computer at the NCAR facility in Boulder, Colorado. The results indicated that using a constant mixing ratio assumption at the top of

the atmosphere and estimates of the ozone values near the surface would give physically realistic results. However the selection of the proper values of the Lagrange multiplier involved considerable numerical experimentation and merits further discussion.

Various weights may be assigned to the second differencing constraint. Because this constraint tends to oppose rapid changes in curvature, it is helpful to weight the constraints at the ends more heavily than the middle, where the solution undergoes more rapid changes in curvature. These typical features may be seen in Fig. 5.1. In this figure, layer one is the top layer in the atmosphere, while layer 78 is the layer immediately above the surface of the earth. All layers have an equal optical depth increment of about 0.01. Notice that the solid curve undergoes rapid changes of curvature in the vicinity of layer ten and also in the vicinity of layer twenty. The other portions of the curve could be closely approximated by a few straight line segments.

One means of relaxing the weights of the constraints is to allow the Lagrange multiplier to vary in magnitude for various depths in the atmosphere. Under these conditions the Lagrange multiplier is no longer a scalar, but now becomes a diagonal matrix. Now Eq. (4.21) becomes

$$((A)^{*}(A)+(\gamma)(H))^{-1}((A)^{*}(E)-(\gamma)(H')(\omega'))=(\omega). \qquad (5.1)$$

Table 5.2

The weighted values of the Lagrange multipliers - for the case where exact intensities are considered.

i	γ_{ii}	i	γ_{ii}	i	γ_{ii}	i	γ_{ii}
1	10^{-5}	6	10^{-8}	11	10^{-8}	16	10^{-7}
2	10^{-5}	7	10^{-8}	12	10^{-8}	17	10^{-5}
3	10^{-5}	8	10^{-8}	13	10^{-8}	18	10^{-5}
4	10^{-5}	9	10^{-8}	14	10^{-8}	19	10^{-5}
5	10^{-8}	10	10^{-8}	15	10^{-8}		

The elements of the diagonal matrix (γ) were reduced by powers of ten to determine the smallest value for each element that is consistent with a physically realistic solution. If the elements of the matrix (γ) were too small, physically unrealistic elements of the solution vector were obtained (i.e. some of the single scattering albedos would either exceed unity or take on negative values). If the elements were chosen to be too large, the resulting solution would give an ozone distribution which resembled some type of gross averaging. In practice each element of the matrix (γ) was reduced until single scattering albedos were observed outside of either the bounds of zero or one. A matrix element a factor of ten larger would then be used. In this way, the original elements of the matrix (γ) were determined on a trial and error basis; however, once the set of Lagrange multipliers was determined, the same set was used for all of the ozone distributions. The diagonal elements of the matrix (γ), the weighted Lagrange multipliers, are presented in Table 5.2 for the case where only numerical errors apply (i.e. the exactly measured intensities were used).

It is necessary to begin the iteration procedure by initially guessing values of the single scattering albedos to be used in the auxiliary equation routine in order to calculate the initially unknown source functions.

Figure 5.4. The inversion results using a single maximum initial guess distribution when the actual distribution possessed a secondary maximum.

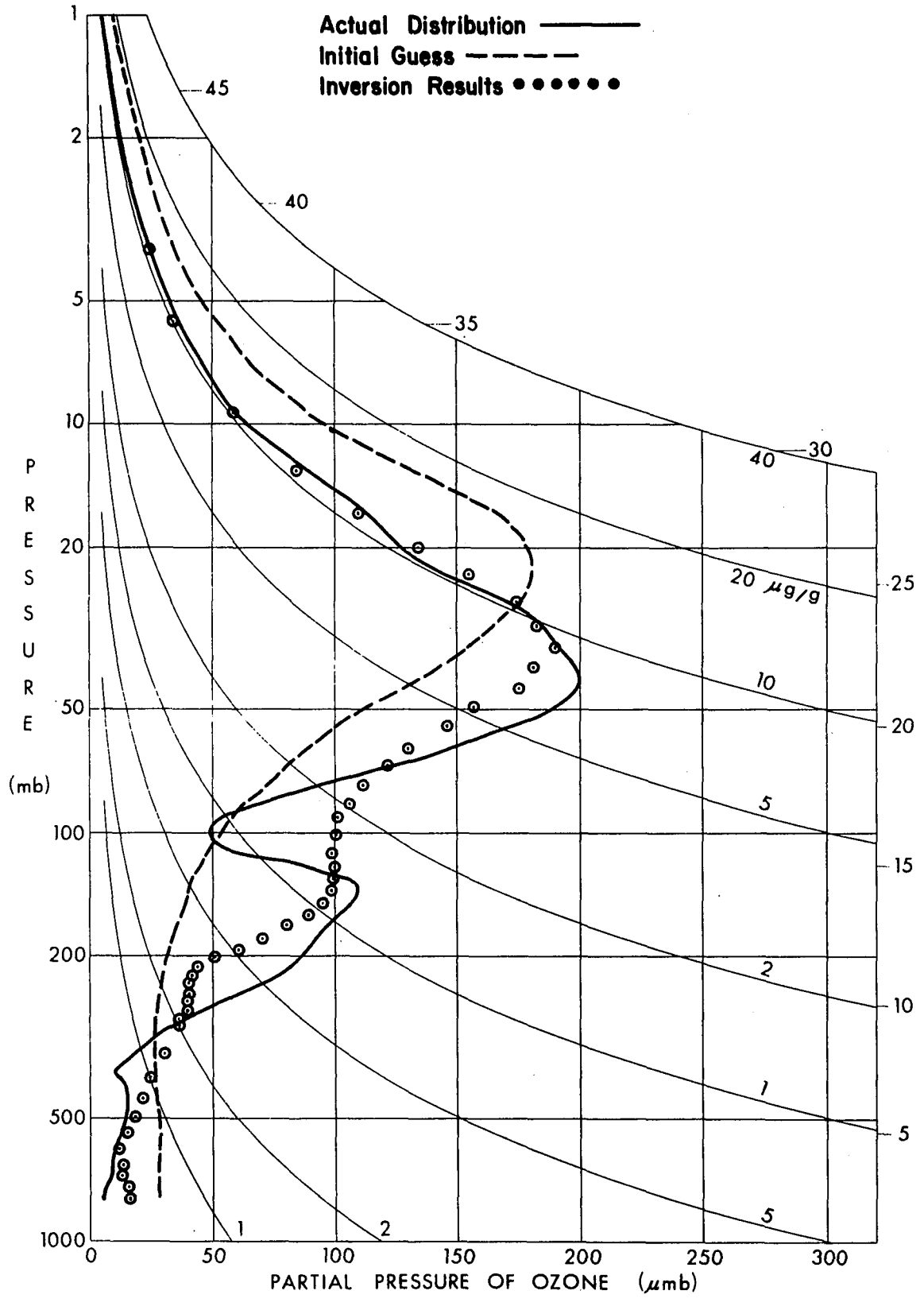
Actual Distribution
Initial Guess
Inversion Results
45
40
35
30
25
20
15
10
5
1
2
20 μg/g
10
5
2
1
5
1
2
PRESSURE (mb)
1
2
5
10
20
50
100
200
500
1000
0
50
100
150
200
250
300
PARTIAL PRESSURE OF OZONE (μmb)

Figure 5.4

Figure 5.5. The inversion results using an initial guess distribution containing a secondary maximum when the actual distribution possessed only a single maximum.

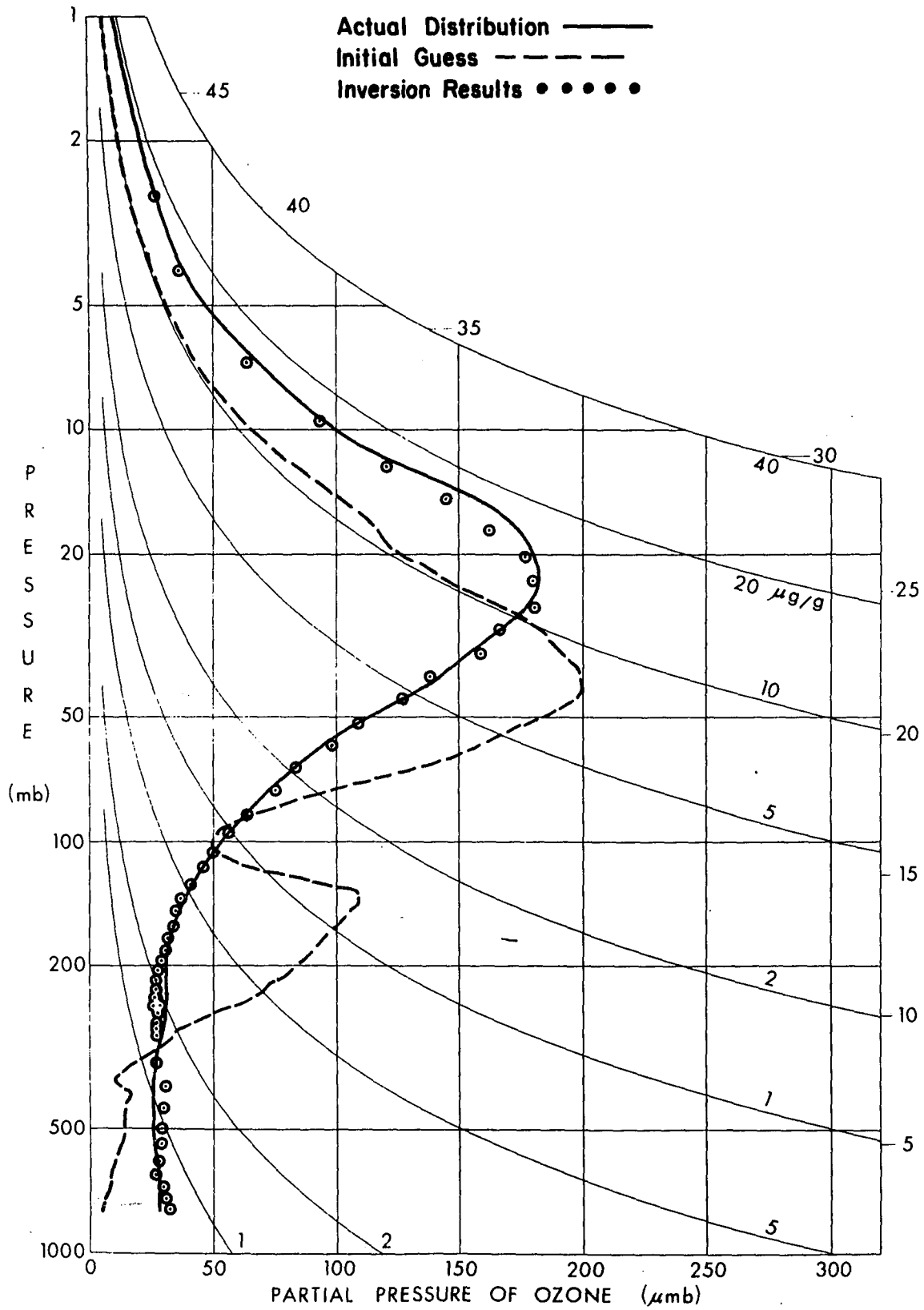
Actual Distribution
Initial Guess
Inversion Results
45
40
35
30
25
20
15
10
5
1
2
20 μg/g
10
5
2
1
5
1
2
PRESSURE (mb)
1
2
5
10
20
50
100
200
500
1000
0
50
100
150
200
250
300
PARTIAL PRESSURE OF OZONE (μmb)

Figure 5.5

It is reasonable to assume that convergence would be achieved more rapidly if the starting distribution is a good approximation to the actual distribution. Hence, in practice, it would seem reasonable to guess initially some standard solution. However, it is essential to know if the solution will also converge to the same results with various initial guesses.

The result of guessing a single hump distribution when the actual distribution has a secondary maximum is shown in Fig. 5.4. Three curves are presented on this figure. The initial guess distribution is indicated by a dashed line, the actual distribution by a solid line and the inversion results are indicated by x's. The points below 300 mb are plotted at 50 mb intervals.

The initial distribution not only has no secondary maximum, but its primary maximum is displaced upward from the actual distribution. The inversion points are in good agreement with the actual distribution down to 30 mb, which is near the primary maximum. The position of the primary maximum is correctly defined along with another important feature in the inversion, the strong indication of a secondary maximum between 100 and 200 mb. As a further test on the validity of this indication of a secondary maximum, the double hump distribution was used as an initial guess, and the single hump distribution was sought. The result of this inversion is shown in Fig. 5.5. Again the position of

the primary maximum is correctly indicated. Also, there is no indication of an unwanted secondary maximum, which implies the secondary maximum indicated in Fig. 5.4 is real and not the result of some numerical instability.

Because further tests indicated that the inversion solution is independent of the choice of the initial guess, a better approximation to the actual solution was used in the following studies in order to speed up the convergence. The method of selecting this initial guess is based on a statistical prediction method (Sellers 1957). This method is presented in Appendix 3.

The results of the inversion for the test dates are shown in Figs. 5.6 to 5.12. Figs. 5.7 to 5.12 have three curves. The solid curves indicate the actual ozone distribution. The circled points, which are the points of interest in the following discussion, represent the inversion results for the condition of zero error in the measured intensities, while the x's represent inversion results when an error was introduced into the measurement. These latter curves will be discussed later. The distribution of ozone from the first data point to the top of the atmosphere is assumed to have a constant mixing ratio as discussed earlier. The remaining points down to the 300 mb level represent the average ozone partial pressure for each Δp. These are plotted for equal optical depth increments ($\sim$0.01) down to

Figure 5.6. Inversion results for Feb. 8, 1964 in terms of single scattering albedos.

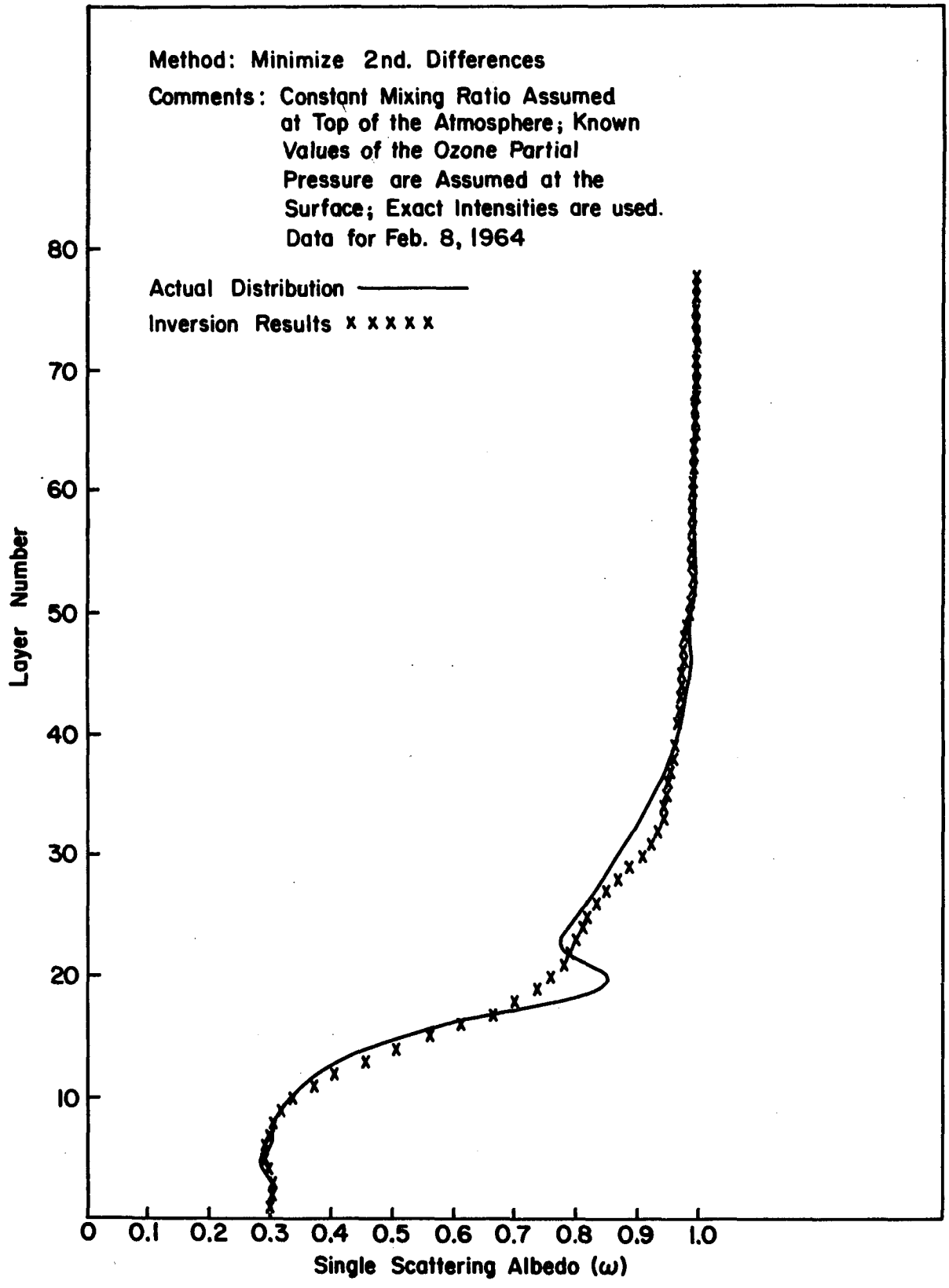
Method: Minimize 2nd. Differences
Comments: Constant Mixing Ratio Assumed at Top of the Atmosphere; Known Values of the Ozone Partial Pressure are Assumed at the Surface; Exact Intensities are used.
Data for Feb. 8, 1964
Actual Distribution
Inversion Results x x x x x
Layer Number
80
70
60
50
40
30
20
10
0
0.1
0.2
0.3
0.4
0.5
0.6
0.7
0.8
0.9
1.0
Single Scattering Albedo (ω)

Figure 5.6

300 mb. The points between 300 mb and the surface are plotted only at 50 mb increments to facilitate plotting.

The inversion results fit the actual curve extremely well at the top of the atmosphere in all six cases. There are two main reasons for this. One reason stems from the fact that the backscattered intensities emergent from the top of the atmosphere are most sensitive to the upper portion of the ozone layer since radiation from lower layers undergoes considerable attenuation. In addition, the slopes of the actual ozone distributions closely follow a constant mixing ratio above the main maximum which is in agreement with the constraint boundary condition. The second differencing constraint also aids the fit in the upper part of the atmosphere, since this constraint discriminates against curvature. The actual values (the solid curve) of the first eight single scattering albedos, as shown in Fig. 5.4, approximately lie on a straight line. This is typical for most ozone distributions. Hence, the second differencing constraint, which is consistent with a constant mixing ratio region, is especially pertinent in this region. A comparison of the inversion results using exact intensities with the actual ozone distribution is shown in Fig. 5.6 in terms of single scattering albedos for Feb. 8, 1964. The solid curve corresponds to the actual ozone distribution and the x's represent the inversion results. Notice that the inversion results smooth out the regions where these are

Figure 5.7. The results of the inversion of intensities with 0% and 1% random errors for Jan. 29, 1964.

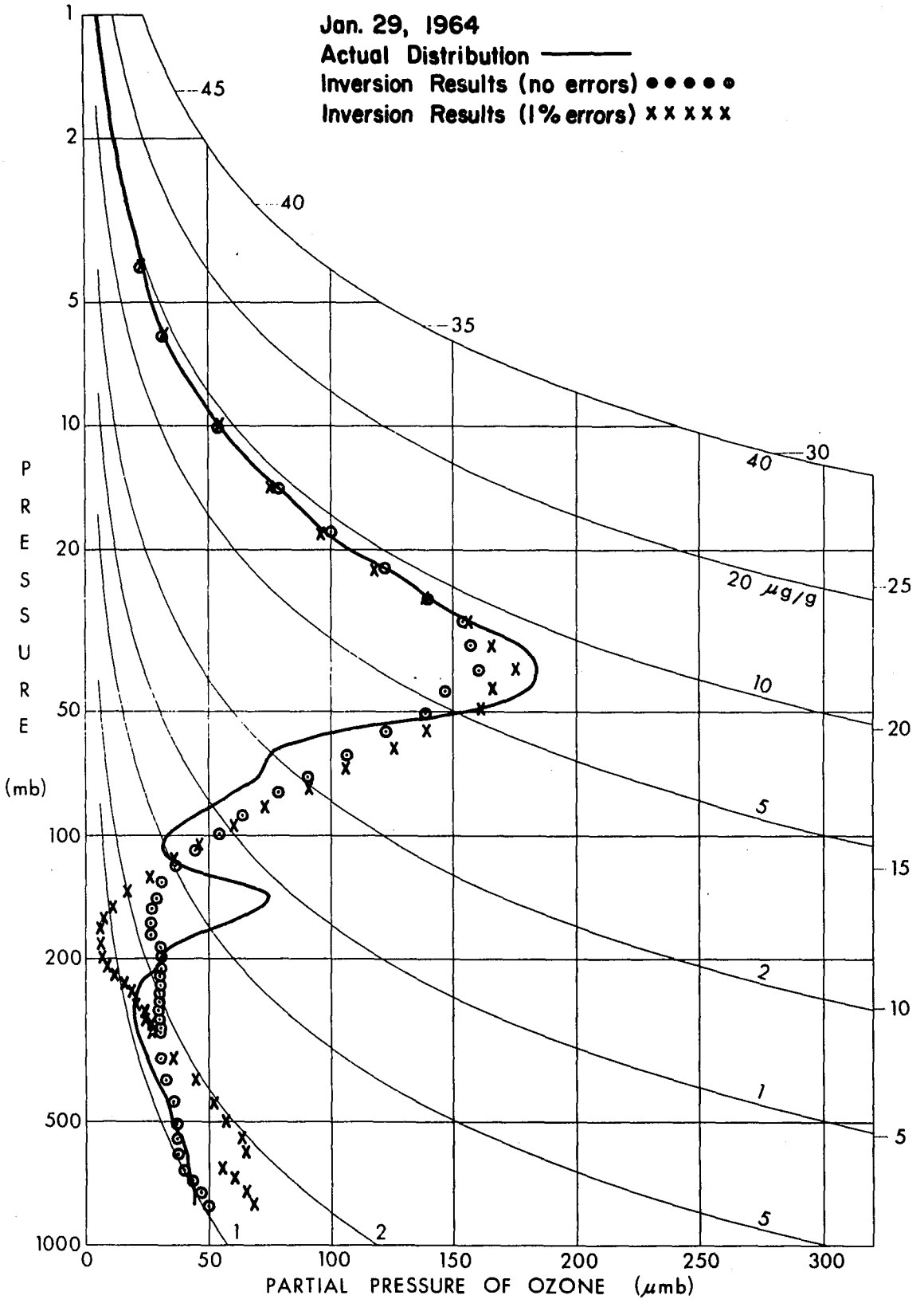
Jan. 29, 1964
Actual Distribution
Inversion Results (no errors)
Inversion Results (1% errors)
45
40
35
30
25
20
15
10
5
20 μg/g
10
5
2
1
5
1
2
PRESSURE (mb)
1
2
5
10
20
50
100
200
500
1000
0
50
100
150
200
250
300
PARTIAL PRESSURE OF OZONE (μmb)

Figure 5.7

Figure 5.8. The results of the inversion of intensities with 0% and 1% random errors for Feb. 7, 1964.

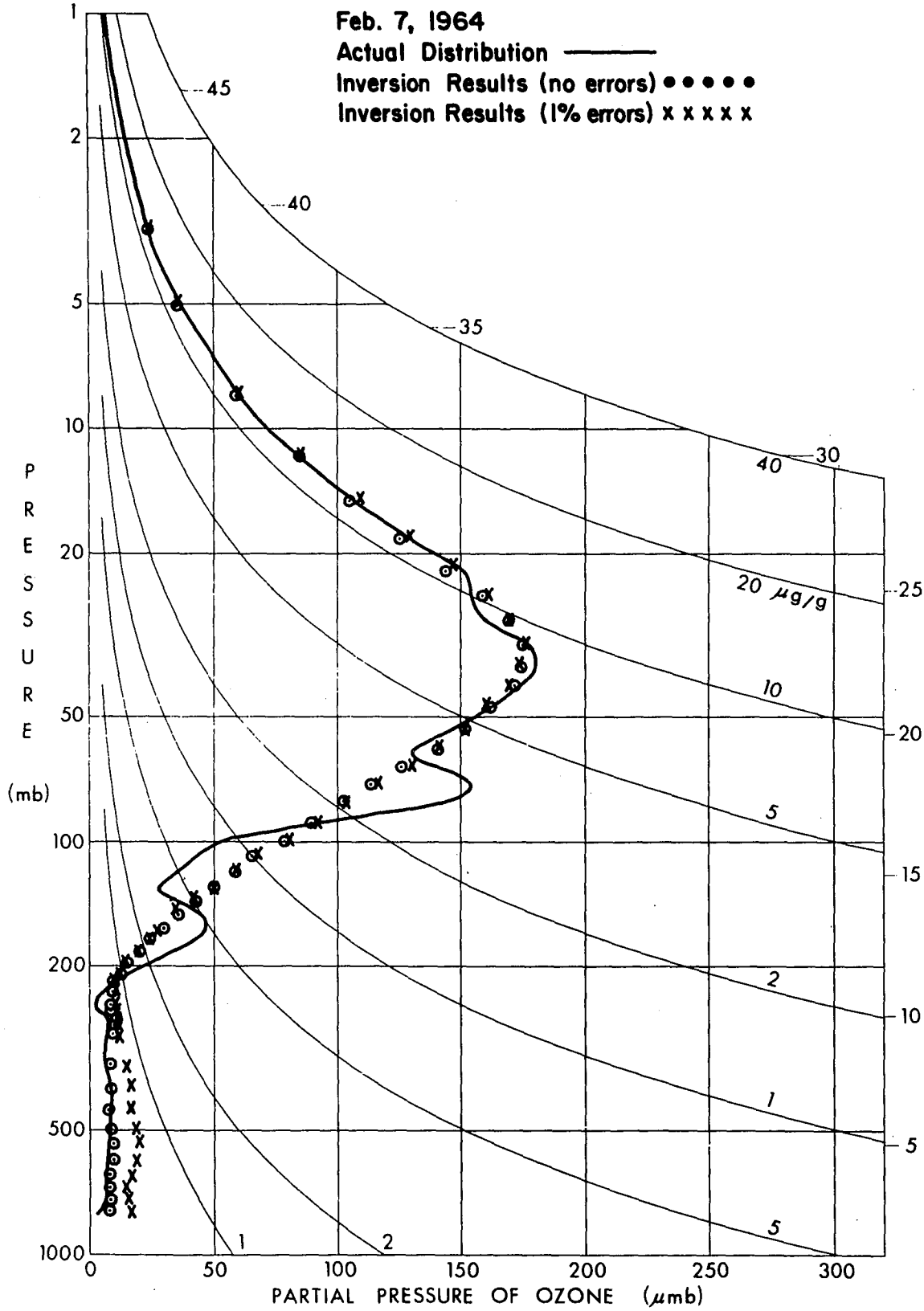
Feb. 7, 1964
Actual Distribution
Inversion Results (no errors) • • • • •
Inversion Results (1% errors) x x x x x
45
40
35
30
25
20
15
10
5
1
2
5
10
20 μg/g
40
PRESSURE (mb)
1
2
5
10
20
50
100
200
500
1000
0
50
100
150
200
250
300
PARTIAL PRESSURE OF OZONE (μmb)

Figure 5.8

Figure 5.9. The results of the inversion of intensities with 0% and 1% random errors for Feb. 8, 1964.

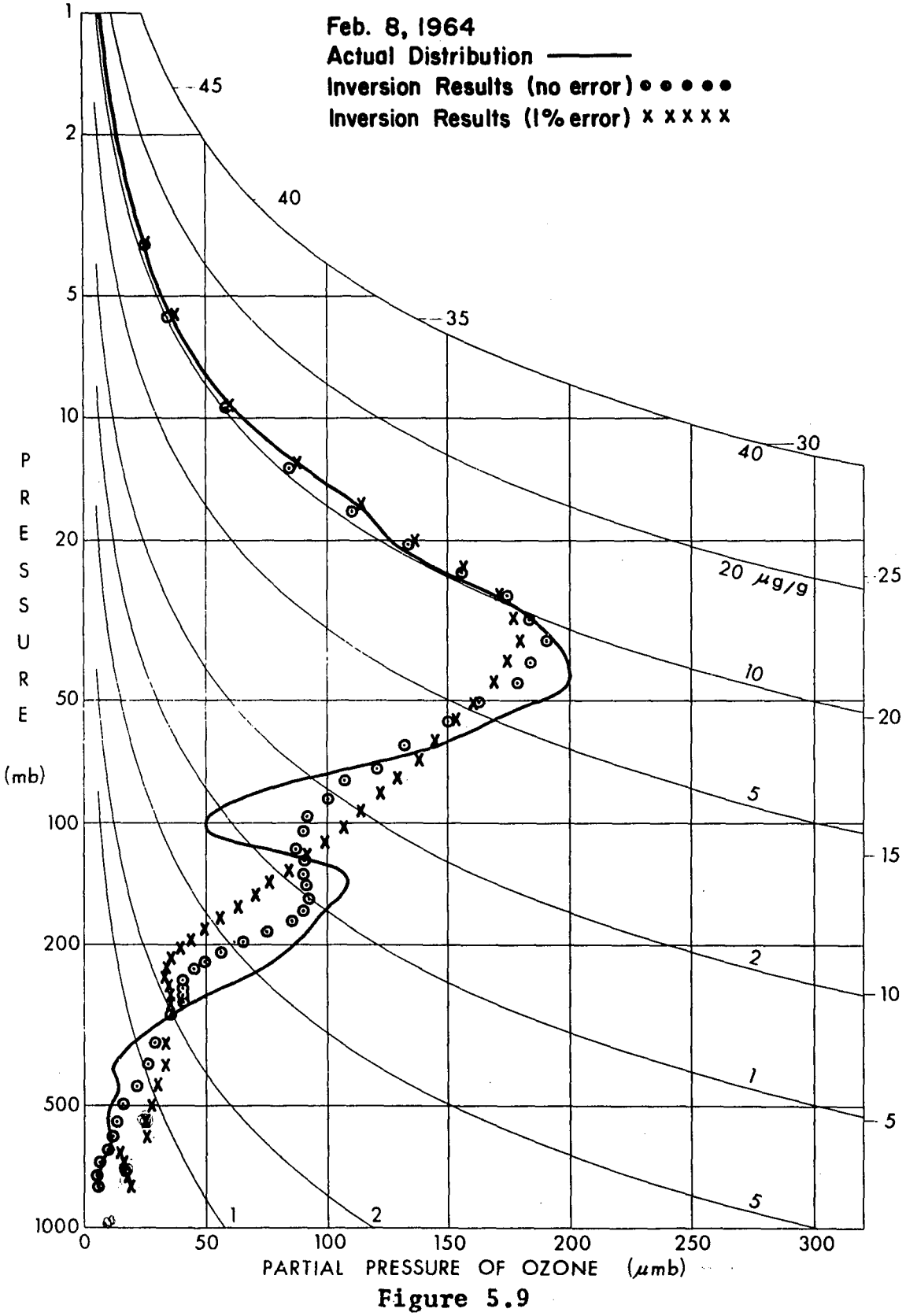
Feb. 8, 1964
Actual Distribution
Inversion Results (no error)
Inversion Results (1% error)
45
40
35
30
25
20
15
10
5
20 μg/g
10
5
2
1
PRESSURE (mb)
1
2
5
10
20
50
100
200
500
1000
0
50
100
150
200
250
300
PARTIAL PRESSURE OF OZONE (μmb)

Figure 5.9

Figure 5.10. The results of the inversion of intensities with 0% and 1% random errors for Feb. 12, 1964.

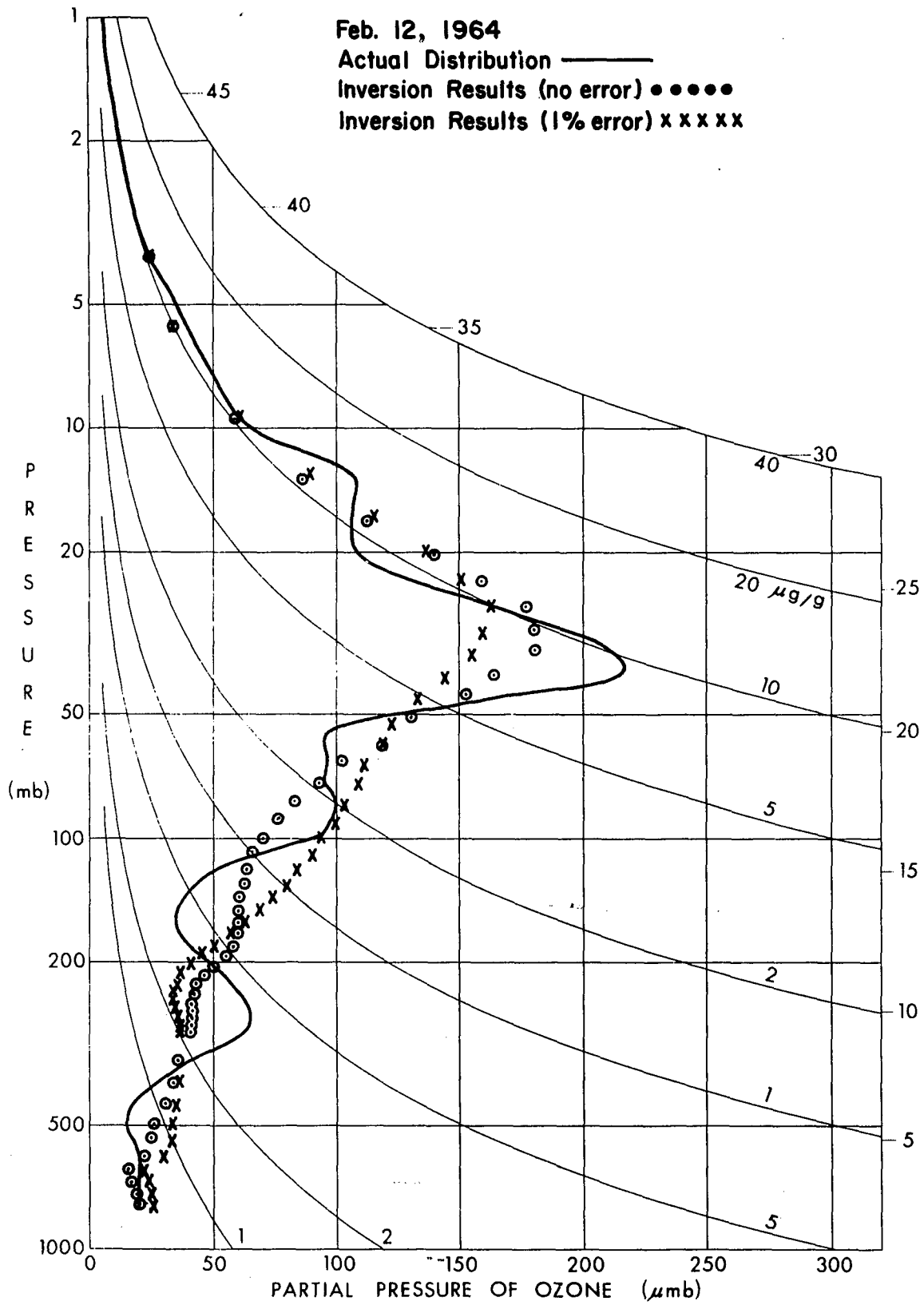
Feb. 12, 1964
Actual Distribution
Inversion Results (no error) ●●●●●
Inversion Results (1% error) x x x x x
45
40
35
30
25
20
15
10
5
20 μg/g
10
5
2
1
PRESSURE (mb)
1
2
5
10
20
50
100
200
500
1000
0
50
100
150
200
250
300
PARTIAL PRESSURE OF OZONE (μmb)

Figure 5.10

Figure 5.11. The results of the inversion of intensities with 0% and 1% random errors for Feb. 17, 1964.

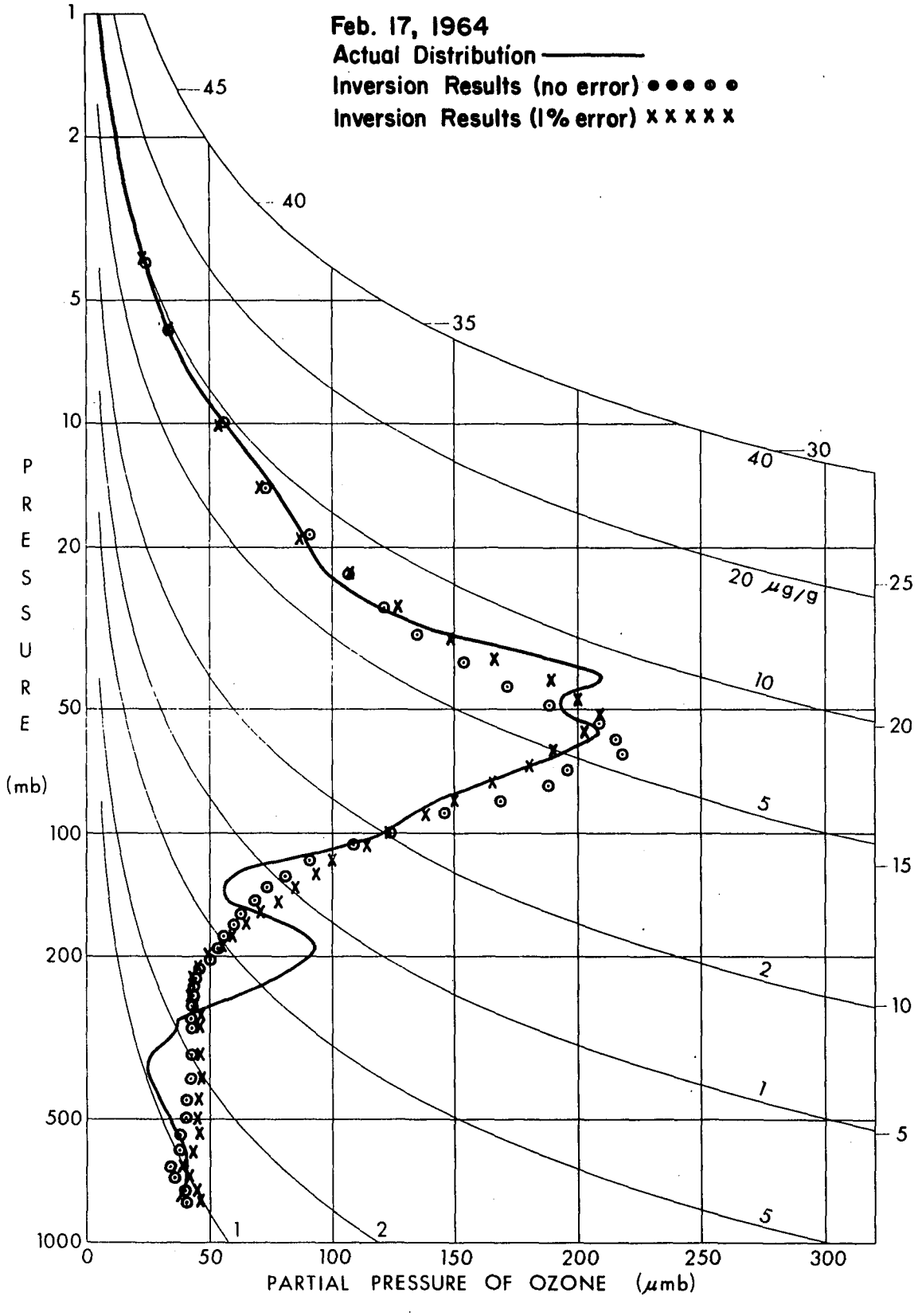
Feb. 17, 1964
Actual Distribution
Inversion Results (no error)
Inversion Results (1% error)
45
40
35
30
25
20
15
10
5
20 μg/g
10
5
2
1
5
2
1
PRESSURE (mb)
1
2
5
10
20
50
100
200
500
1000
0
50
100
150
200
250
300
PARTIAL PRESSURE OF OZONE (μmb)

Figure 5.11

Figure 5.12. The results of the inversion of intensities with 0% and 1% random errors for Feb. 20, 1964.

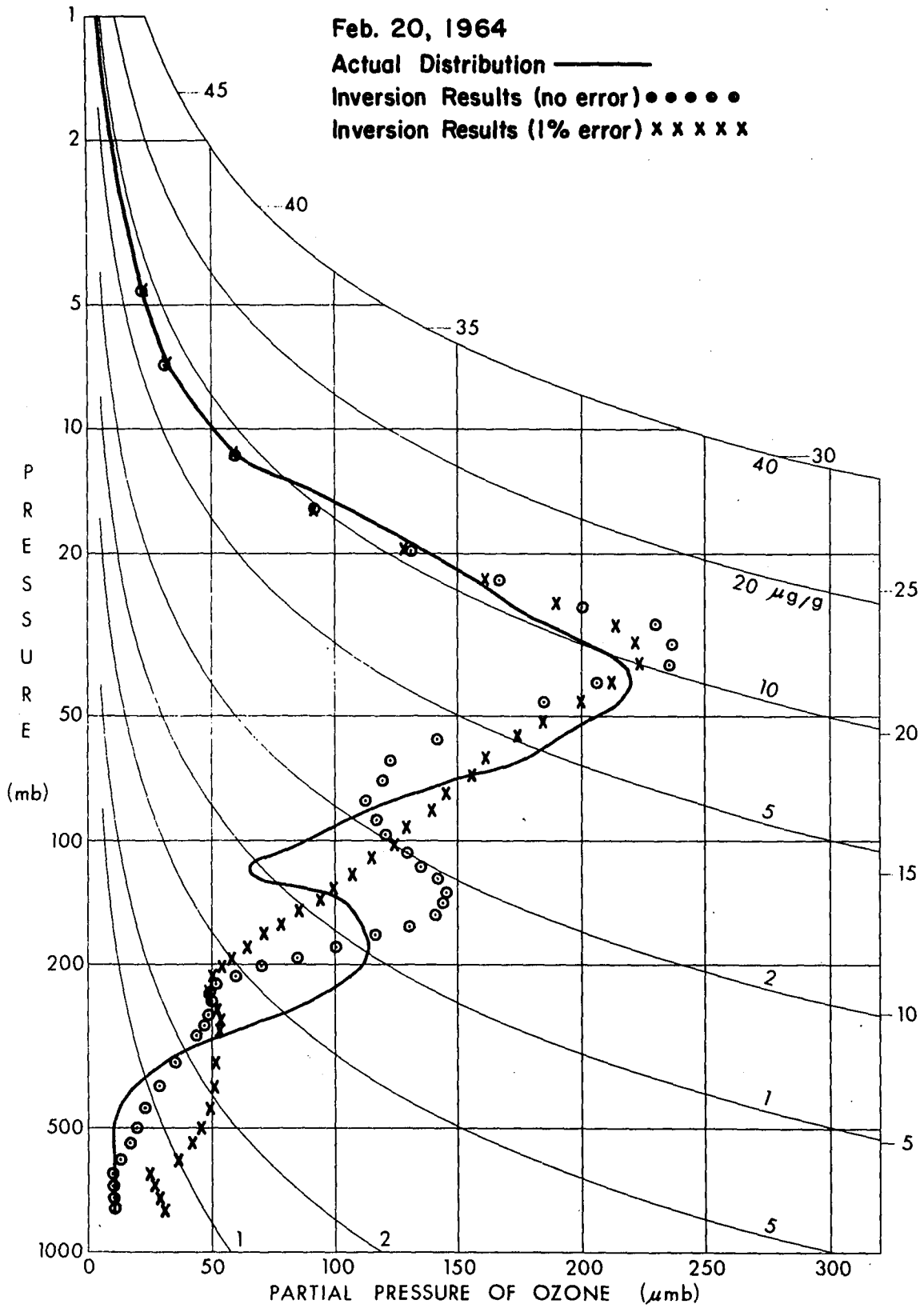
Feb. 20, 1964
Actual Distribution ———
Inversion Results (no error) • • • • •
Inversion Results (1% error) x x x x x
45
40
35
40
30
20 μg/g
25
10
20
5
15
2
10
1
5
5
1
2
PRESSURE (mb)
1
2
5
10
20
50
100
200
500
1000
0
50
100
150
200
250
300
PARTIAL PRESSURE OF OZONE (μmb)

Figure 5.12

large variations over a few layers. Another important feature is the good agreement in the slopes of the two curves when the slope is relatively constant for several layers. Both of these features are consistent with the constraint which requires that the square of the second difference be a minimum.

The primary maximum is, in general, reproduced quite well. The best fit of the data points in the vicinity of the maximum to the actual curve occurs in Figs. 5.7, 5.8 and 5.9. These ozone distributions have relatively broad peaks, hence the constraint of minimizing the second differences discriminates less against these curves than for the distributions with sharper primary maxima (see Fig. 5.10, 5.11 and 5.12). It appears that the peak is well defined if the portion of the ozone distribution above the curve closely follows a constant mixing ratio line. Compare Figs. 5.7, 5.8, 5.9 and 5.10 with Figs. 5.11 and 5.12. These data indicate that deviations from a constant mixing ratio in the upper portion of the ozone distribution (e.g. Figs. 5.11 and 5.12) influence the position of the primary maxima since the second differencing constraint causes persistence in the slope of the single scattering albedos. This means that early trends in the upper portion of the ozone distribution toward smaller mixing ratios (e.g. Fig. 5.11) will result in a primary maximum displaced below the proper position and conversely, increasing ozone

mixing ratios in the portion of the curve above the main maximum (e.g. Fig. 5.12) will displace the inversion solution above the actual curve.

The remarkable fit of the inversion points to the actual curve near the bottom of the ozone distribution is not entirely justified. Because one often has a good feeling for typical values of surface ozone amounts one can build this information into the constraint at the bottom (see Chapter IV). In these six curves the actual value at the ground was used instead of some uniform average value. Hence, the fit is better than could be expected in practice. It appears that 25 or 30 mb would have been a good average value to use in these distributions.

The absence of extraneous features that result from numerical instabilities is indicated by Figs. 5.7 and 5.8. The actual curves have only very minor secondary humps. Any indication of these features would be very suspicious since there is very little information in the backscattered intensities from these lower layers. The absence of minor humps in these two distributions is, in this sense, significant. An upper hump above the primary maximum in the actual distribution is not indicated by the inversion data points in Fig. 5.10. This curve is a good example of the amount of smoothing that is accomplished by the inversion

technique. The secondary hump below the main maximum is probably real, in the sense that it is the result of a gross smoothing of the humps at 80 and 260 mb. Gross secondary features, such as the lower hump shown in Figs. 5.9 and 5.12, show up in the inversion technique. However, it will be seen that even these features are lost when measurement errors are considered. As previously discussed, the total amount of ozone is assumed independently known in the inversion routine. The inversion routine considers the total optical depth as constant, but the relative values of the total scattering and absorption optical depths (and therefore the total ozone amount and the surface pressure) are allowed to vary in a manner consistent with this constraint and the results of the inversion. A means of checking the validity of the inversion may be accomplished by comparing the total amount of ozone, as determined from the single scattering albedos that result from the inversion, with the independently determined total ozone amount used in the initial optical depth calculation. These comparisons are shown in Table 5.3. As can be seen, the agreement between the actual total ozone amounts and the inversion results are very good.

Table 5.3

Total Ozone (m atm-cm)

Date	Actual	Inversion
Jan. 29, 1964	297	297
Feb. 7, 1964	330	329
Feb. 8, 1964	369	367
Feb. 12, 1964	340	341
Feb. 17, 1964	374	372
Feb. 20, 1964	398	398

The Effects of Random Errors.

In order to establish the effect of random measurement errors on the inversion procedure, 1% random errors were introduced into the intensities emergent from the top of the atmosphere in the following manner. The CDC 6600 computer at the NCAR facility has an internal subroutine that generates random numbers between zero and one. A random number was generated for each of the simulated measured intensities. If the value of the random number was less than 0.5 the intensity was multiplied by 0.99, and if the random number was greater than 0.5 the intensity was multiplied by 1.01. The ozone distributions obtained from intensities containing 1% random errors are indicated by x's in Figs. 5.7 and through 5.12. For these curves the magnitudes of the weighted Lagrange multipliers were necessarily increased to overcome the numerical oscillations that would dominate the solution. The diagonal elements of the matrix (γ) (i.e. the weighted Lagrange multipliers) are listed in Table 5.4. These Lagrange multipliers must be consistent with the *a priori* error estimates as discussed earlier. The reflected intensities have values on the order of 10^{-2}, therefore the 1% errors must be on the order of 10^{-4}. Since there are sixty values of the reflected intensities, the sum of the errors squared will be approximately 6×10^{-7}. The actual sum of the errors squared as

determined from Eq. (3.1) is 0.5×10^{-7}. This agreement is considered satisfactory.

Table 5.4

The weighted values of the Lagrange multipliers - for the cases where 1% random errors are introduced into the intensities.

i	γ_{ii}	i	γ_{ii}	i	γ_{ii}	i	γ_{ii}
1	10^{-5}	6	10^{-7}	11	10^{-6}	16	10^{-4}
2	10^{-5}	7	10^{-7}	12	10^{-5}	17	10^{-4}
3	10^{-5}	8	10^{-6}	13	10^{-5}	18	10^{-4}
4	10^{-5}	9	10^{-6}	14	10^{-5}	19	10^{-4}
5	10^{-7}	10	10^{-6}	15	10^{-4}		

There is now no evidence of a secondary maximum in any of the figures. These distributions, based on values of intensities with 1% errors are, however, still good approximations to the actual distributions. The positions of the primary maxima are good in general, although the effect of minimizing second differences shows up again in Figs. 5.11 and 5.12. The distributions which gave no evidence of a secondary maximum with no errors in the "measured" intensities (Figs. 5.7, 5.8, 5.11) show very little change when the 1% errors were introduced. However, the distributions which indicated the existence of a secondary maximum (Figs. 5.9, 5.10 and 5.12) show an

averaging throughout the layer where the secondary maximum previously occurred. Again the positions of the points in the upper portion of the curve show very little change. The expected displacement of the points due to the 1% errors is apparently damped out by the smoothness constraint. There is considerable evidence of a lack of information in the bottom portion of the curves. The differences from the actual curves increase considerably in this region. The discontinuity that is apparent in all figures in the last few points is a numerical effect which results from grouping several layers at the bottom and requiring that they have the same ozone mixing ratio.

Another error is introduced by the initial assumption in the inversion process that the earth and its atmosphere could be approximated as plane-parallel. The orbits of the first TIROS satellites (I-IV) were circular at a 400-n mi altitude (Rados 1967). At this altitude the angle between the tangent point on the earth and the nadir is about 64°. If an orbit of 150 n-mi could be achieved, this angle would be increased to about 74°. As one scans beyond the tangent point of the earth, sphericity effects are very likely to become increasingly important. Due to mathematical complexities, the effects of sphericity are difficult to assess when multiple scattering and polarization are considered, hence it was decided to attempt inversions when only angles less than 74° were considered.

Figure 5.13. The results of the inversion of exact intensities for Feb. 8, 1964 where observation angles less than 74 degrees were used.

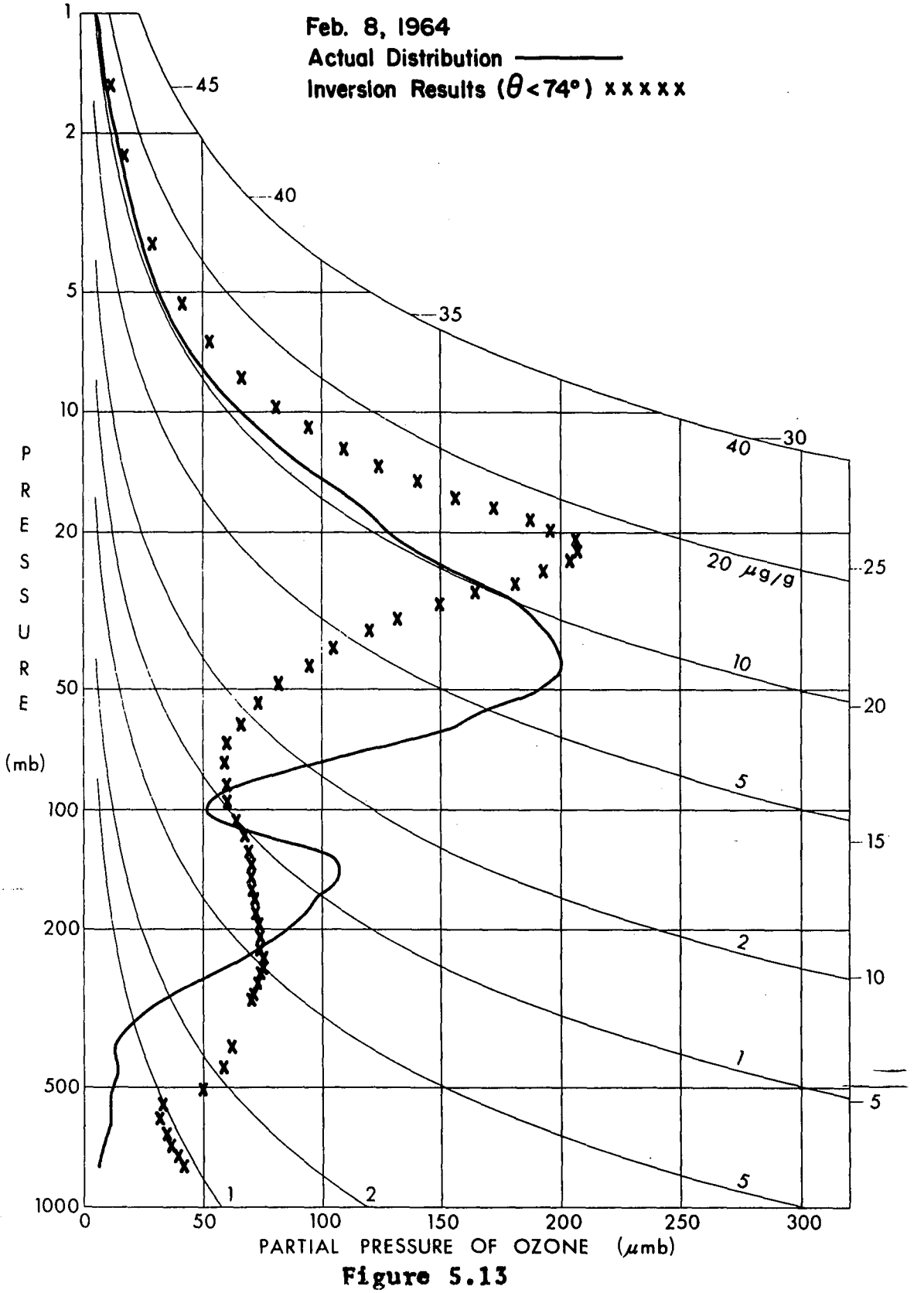
Feb. 8, 1964
Actual Distribution
Inversion Results (θ<74°) x x x x x
45
40
35
30
25
20
15
10
5
20 μg/g
10
5
2
1
1
2
5
P
R
E
S
S
U
R
E
(mb)
1
2
5
10
20
50
100
200
500
1000
0
50
100
150
200
250
300
PARTIAL PRESSURE OF OZONE (μmb)

Figure 5.13

The angles used are listed in Table 5.5. In addition to requiring that the angles are less than 74 degrees, the angles with one exception, have been chosen at four degree intervals. The one exception is the increment between three and six degrees. These angles would be easier to achieve in an actual instrument system than those listed in Table 5.1.

Table 5.5

Angles between the tangent point on the earth and the nadir. Here $\mu=\cos\theta$ where θ is the angle from the nadir.

μ	θ	μ	θ	μ	θ
.27563	74°	.69466	46°	.95106	18°
.34202	70°	.74314	42°	.97030	14°
.40674	66°	.78801	38°	.98481	10°
.46947	62°	.82904	34°	.99452	6°
.52991	58°	.86603	30°	.99863	3°
.58779	54°	.89879	26°		
.64279	50°	.92718	22°		

Even when the exact values of the simulated measured intensities were used for this case, the inversion results were very poor. An example of the type of results obtained under these conditions is shown in Fig. 5.13. The solid line in this figure is the actual distribution for Feb. 8, 1964. The inversion results, the x's, show little resemblence to the actual distribution except in the first few points

near the top of the curve. The available information correctly specifies these first few points but there apparently is insufficient information from the lower layers of the atmosphere to determine even approximately the main maximum. That the reason for this stems from a lack of information can be demonstrated from an inspection of the eigenvalues of the (A)*(A) matrix. From Chapter III we have the result that there is a degree of independence in our system of equations for each eigenvalue that satisfies Eq. (3.17). Eigenvalues for data corresponding to Feb. 8, 1964 are listed in Table 5.6. The eigenvalues for both no errors and 1% random errors in the intensities at the angles listed in Table 5.1 are shown, as are the eigenvalues for the case of exact intensities corresponding to the observation angles listed in Table 5.5. The sums of the squares of the errors divided by the number of angles are also listed for each of the three cases. From the condition stated by Eq. (3.17), there is a degree of independence for each eigenvalue that is significantly larger than the sum of the errors squared divided by the total number of single scattering albedos sought. One can see from Table 5.6 that there are at most eight eigenvalues which satisfy this condition for the case of no measurement errors and angles beyond the limit of the earth, Case I; six eigenvalues for the same geometry but 1% random errors, Case II; and only four eigenvalues are significant for the

Table 5.6

Eigenvalues and Sums of Errors Squared.

Eigenvalues are presented for 0% and 1% random errors in the measured intensities which correspond to the angles listed in Table 5.1. Eigenvalues are also presented for exact values of the measured intensities which correspond to the angles listed in Table 5.5. The data are presented for Feb. 8, 1964. The sums of the errors squared divided by the number of layers in the inversion scheme are presented at the bottom for each case. The number in each parenthesis is the power of ten by which the preceding number is to be multiplied.

N	no errors (see Table 5.1)	1% errors	no errors (see Table 5.5)	N	no errors (see Table 5.1)	1% errors	no errors (see Table 5.5)
1	.97646(-2)	.97965(-2)	.35477(-2)	11	.10351(-10)	.43108(-11)	.97730(-12)
2	.35408(-2)	.37118(-2)	.16170(-3)	12	.92299(-11)	.31250(-11)	.59580(-12)
3	.72949(-3)	.74546(-3)	.17843(-5)	13	.86916(-11)	.30592(-11)	.22061(-12)
4	.89176(-4)	.91278(-4)	.51111(-7)	14	.32420(-11)	.27731(-11)	.11141(-12)
5	.10522(-4)	.10919(-4)	.18568(-8)	15	.24820(-11)	.24776(-11)	.98783(-13)
6	.67483(-6)	.69815(-6)	.34284(-9)	16	.23539(-11)	.17931(-11)	.92968(-13)
7	.22788(-7)	.22681(-7)	.16235(-11)	17	.21609(-11)	.17068(-11)	.64675(-13)
8	.59544(-9)	.58792(-9)	.13479(-11)	18	.14787(-11)	.11812(-11)	.43750(-13)
9	.39523(-10)	.59420(-10)	.13087(-11)	19	.63269(-12)	.49273(-12)	.15724(-13)
				$\frac{\sum_{i=1}^{19} \epsilon_i^2}{N}$	.9(-10)	.5(-7)	.6(-8)

case of no measurement errors but observation angles restricted to values less than 74 degrees, case III.

These results do not mean, for example, that the ozone distributions obtained under the conditions of Case I could have been determined equally as well by using only eight layers. The eigenvalues were determined only on the basis of the matrix (A)*(A); however, additional information is used in the solutions. The constant mixing ratio assumption at the top of the ozone distribution and the estimate of the average value of the surface ozone furnished additional information concerning the end points. Also, the smoothness constraint puts bounds on the overall shape of the distribution. It must be concluded however, that an important means of evaluating the amount of information available for the inversion is furnished by an eigenvalue analysis.

CHAPTER VI

A COMPARISON OF VARIOUS METHODS FOR DETERMINING THE VERTICAL OZONE DISTRIBUTION

The Statistical Method.

A statistical prediction method which is based on work done by Sellers (1957) is presented in Appendix 3. The results of this statistical study showed that for the period selected (i.e. January and February during 1964, 1965 and 1966), and for the predictors considered (see Table A-3.1), the only parameter significantly correlated with the vertical ozone distribution was the total ozone amount. The results of using only the total amount of ozone to predict the vertical ozone distributions for the previously selected dates are shown in Figs. 6.1 through 6.6. Four curves are presented in each of these figures. The curves of immediate interest, those corresponding to the statistical distribution, are indicated by dotted lines, the actual distributions are indicated by dot and dashed lines, the inversion results are indicated by x's and the Umkehr block distributions are indicated by solid lines. A readily apparent feature among these curves is the strong similarity in their general shapes. The maximum values of the ozone partial pressure at the primary maxima vary, but the positions of these maxima all occur near 40 mb. The actual

Figure 6.1. A comparison of the vertical ozone distribution obtained from an ozonesonde, the Dütsch-Mateer Umkehr method, a statistical method, and the inversion of intensities with 1% random errors for Jan. 29, 1964.

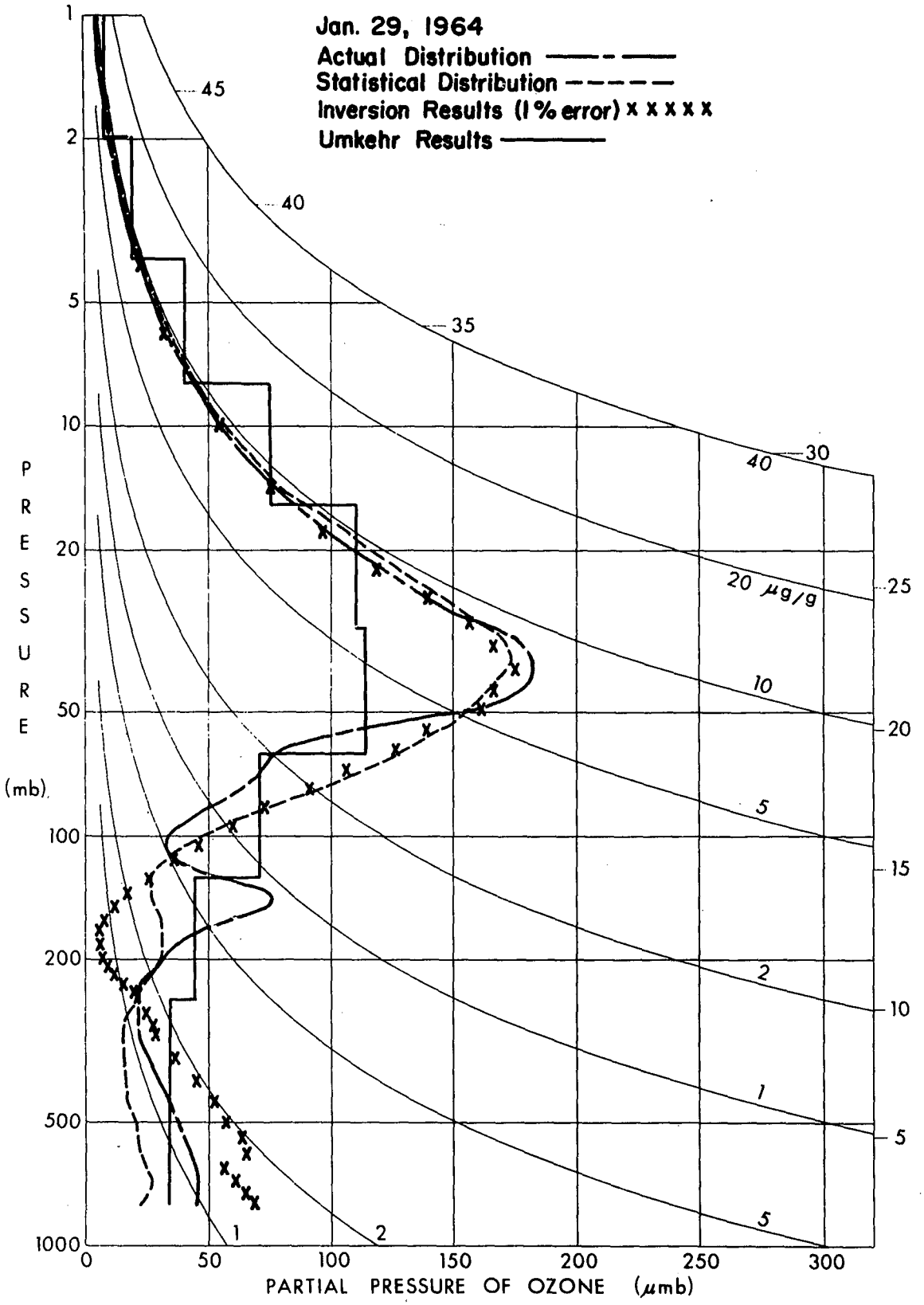
Jan. 29, 1964
Actual Distribution
Statistical Distribution
Inversion Results (1% error) x x x x x
Umkehr Results
45
40
35
30
25
20
15
10
5
40
20 μg/g
10
5
2
1
5
1
2
PRESSURE (mb)
1
2
5
10
20
50
100
200
500
1000
0
50
100
150
200
250
300
PARTIAL PRESSURE OF OZONE (μmb)

Figure 6.1

Figure 6.2. A comparison of the vertical ozone distributions obtained from an ozonesonde, the Dütsch-Mateer Umkehr method, a statistical method, and the inversion of intensities with 1% and random errors for Feb. 7, 1964.

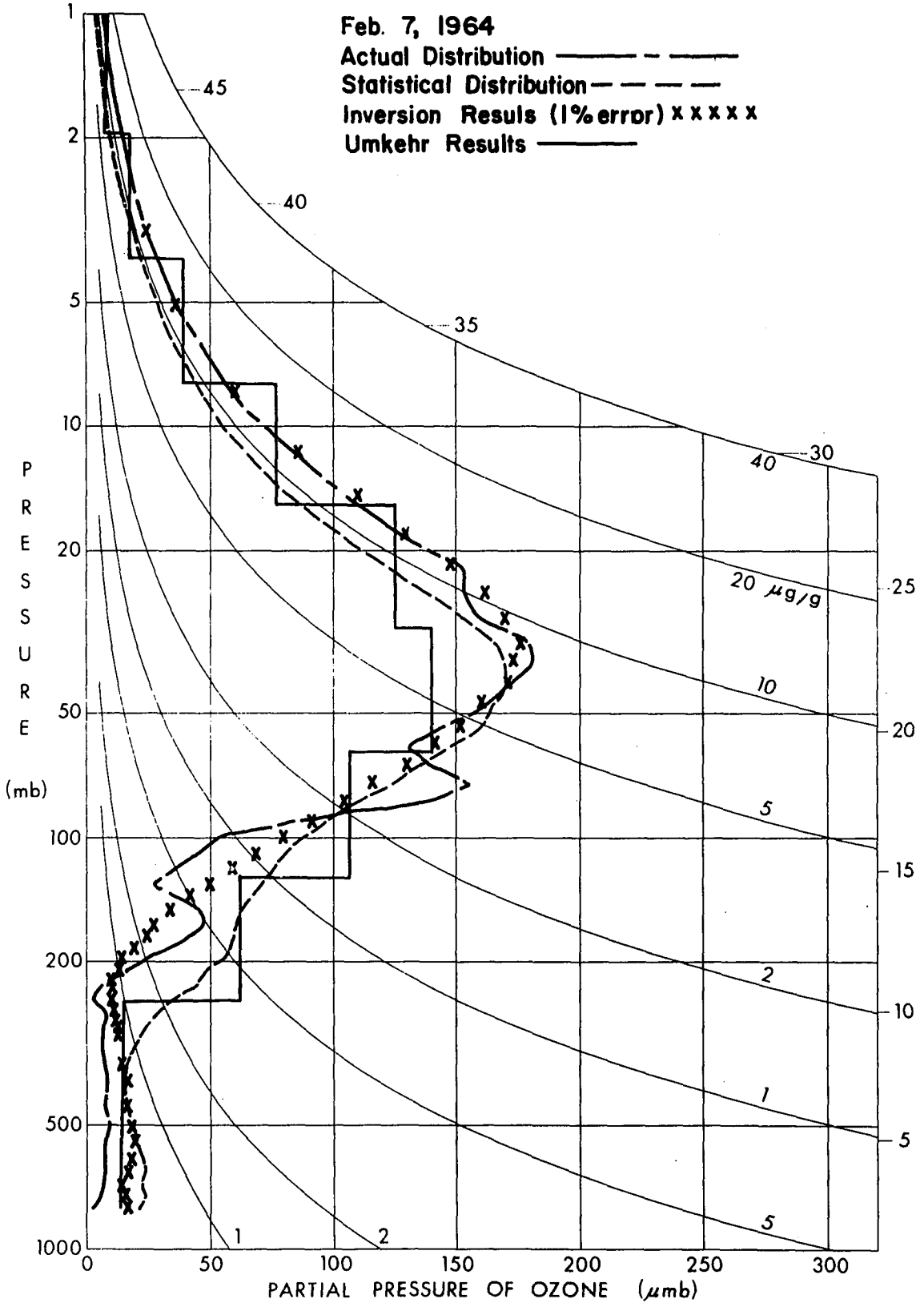
Feb. 7, 1964
Actual Distribution
Statistical Distribution
Inversion Resuls (1% error) x x x x x
Umkehr Results
45
40
35
30
25
20
15
10
5
40
20 μg/g
10
5
2
1
5
1
2
1
2
5
10
20
50
100
200
500
1000
PRESSURE (mb)
0
50
100
150
200
250
300
PARTIAL PRESSURE OF OZONE (μmb)

Figure 6.2

Figure 6.3. A comparison of the vertical ozone distributions obtained from an ozonesonde, the Dütsch-Mateer Umkehr method, a statistical method, and the inversion of intensities with 1% random errors for Feb. 8, 1964.

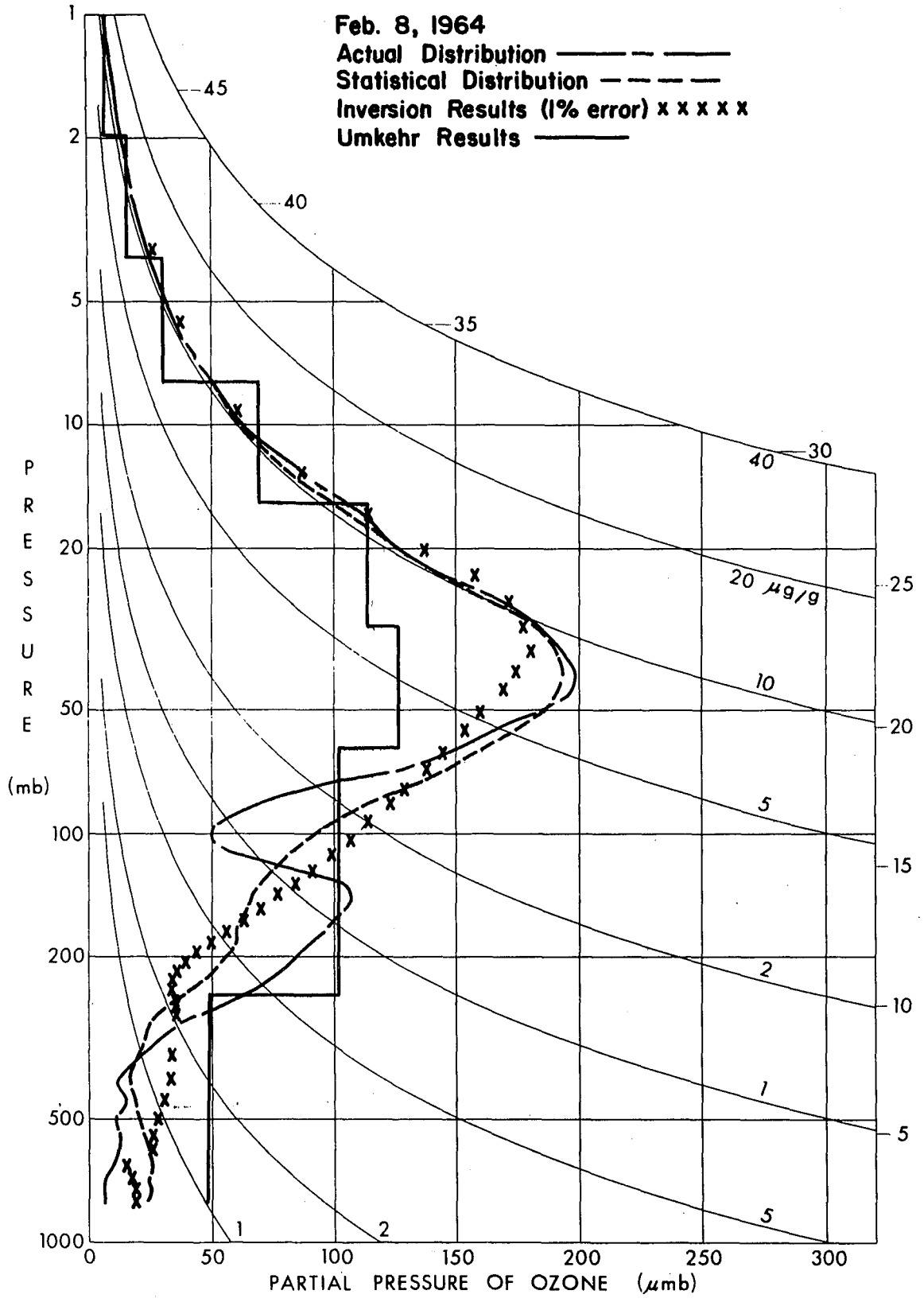
Feb. 8, 1964
Actual Distribution
Statistical Distribution
Inversion Results (1% error) x x x x x
Umkehr Results
45
40
35
30
25
20
15
10
5
40
20 μg/g
10
5
2
1
5
1
2
P
R
E
S
S
U
R
E
(mb)
1
2
5
10
20
50
100
200
500
1000
0
50
100
150
200
250
300
PARTIAL PRESSURE OF OZONE (μmb)

Figure 6.3

Figure 6.4. A comparison of the vertical ozone distributions obtained from an ozonesonde, the Dütsch-Mateer Umkehr method, a statistical method, and the inversion of intensities with 1% random errors for Feb. 12, 1964.

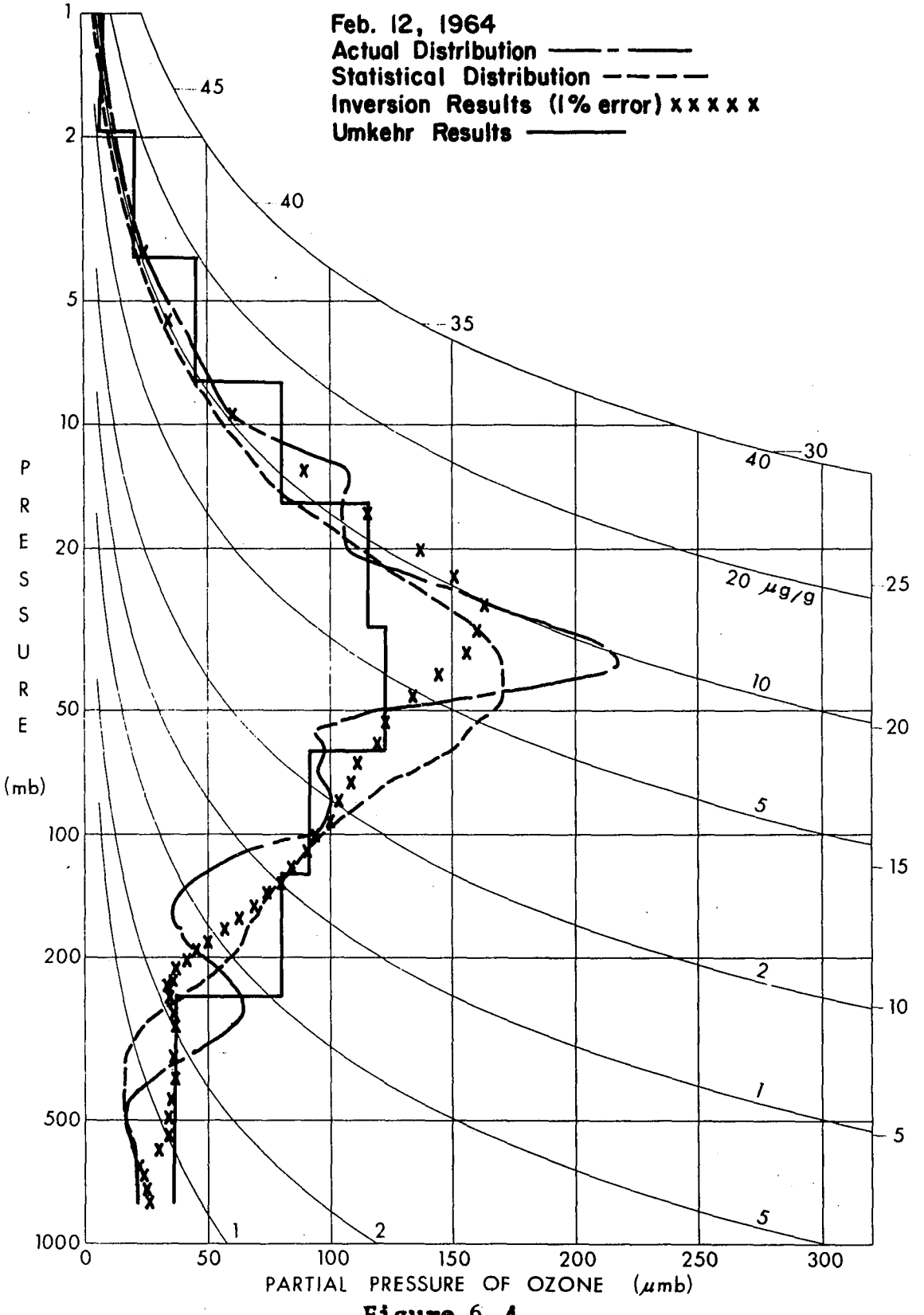
Feb. 12, 1964
Actual Distribution
Statistical Distribution
Inversion Results (1% error) x x x x x
Umkehr Results
45
40
35
30
25
20
15
10
5
20 μg/g
10
5
2
1
5
1
2
PRESSURE (mb)
1
2
5
10
20
50
100
200
500
1000
0
50
100
150
200
250
300
PARTIAL PRESSURE OF OZONE (μmb)

Figure 6.4

Figure 6.5. A comparison of the vertical ozone distributions obtained from an ozonesonde, the Dütsch-Mateer Umkehr method, a statistical method, and the inversion of intensities with 1% random errors for Feb. 17, 1964.

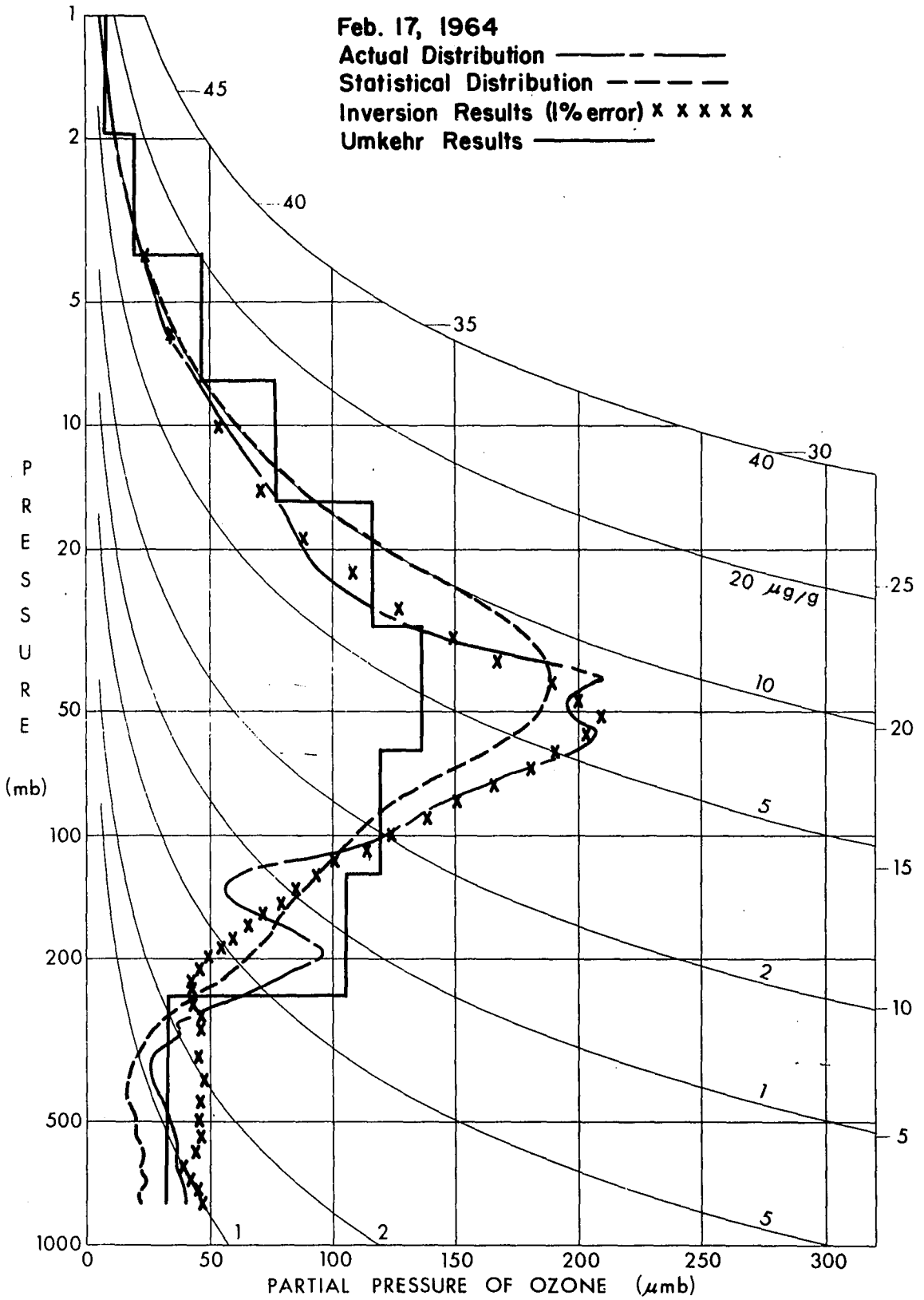
Feb. 17, 1964
Actual Distribution
Statistical Distribution
Inversion Results (1% error) x x x x x
Umkehr Results
45
40
35
30
25
20
15
10
5
20 μg/g
10
5
2
1
5
PRESSURE (mb)
1
2
5
10
20
50
100
200
500
1000
0
50
100
150
200
250
300
PARTIAL PRESSURE OF OZONE (μmb)

Figure 6.5

Figure 6.6. A comparison of the vertical ozone distributions obtained from an ozonesonde, the Dütsch-Mateer Umkehr method, a statistical method, and the inversion of intensities with 1% random errors for Feb. 29, 1964.

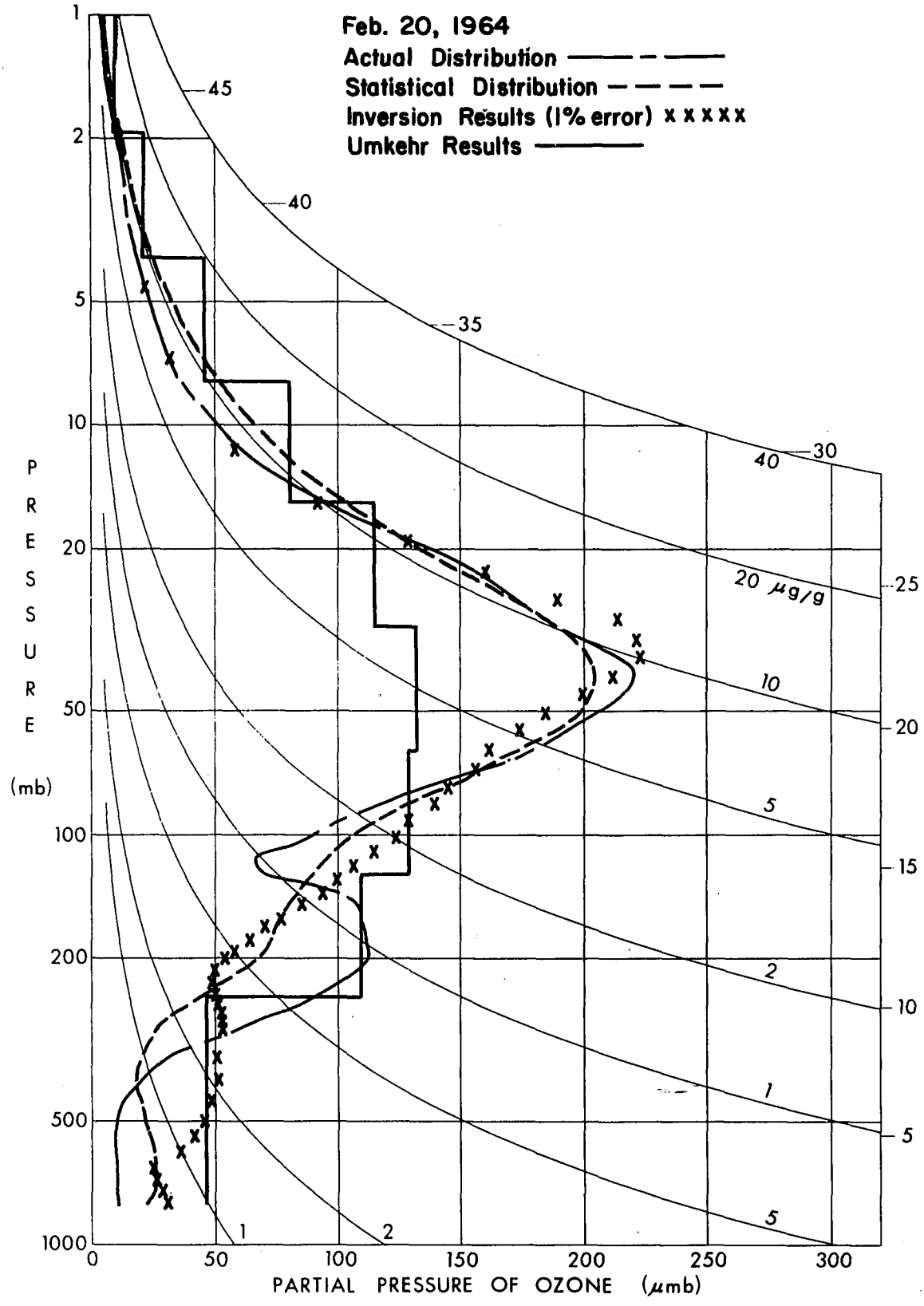
Feb. 20, 1964
Actual Distribution
Statistical Distribution
Inversion Results (1% error) x x x x x
Umkehr Results
45
40
35
30
25
20
15
10
5
20 μg/g
10
5
2
1
5
1
2
PRESSURE (mb)
1
2
5
10
20
50
100
200
500
1000
0
50
100
150
200
250
300
PARTIAL PRESSURE OF OZONE (μmb)

Figure 6.6

maximum is higher in Fig. 6.4 and lower in Fig. 6.5, hence the agreement with the statistical predictions is relatively poor for these curves. The agreement with the actual curves in the upper portion of the curves, above the primary maximum, is only fair. This is particularly noticeable in Figs. 6.2, 6.5 and 6.6. An indication of a secondary hump is present in all figures. However, this results from the typical presence of this feature in a large number of cases for the period of the sample.

These statistical distributions were used as first guesses in the inverse procedure. Because they do appear to be good general approximations to the actual curves, the number of iterations that are required for convergence is reduced from those that would be required from a more arbitrary choice, although, as discussed earlier, any initial distribution would lead to the same results.

The Umkehr Method.

A detailed description of an objective Umkehr evaluation procedure has been described by Mateer (1964) and Mateer and Dütsch (1964). The results of applying this Umkehr evaluation procedure to observations from the world ozone network have been reported by Dütsch and Mateer (1964). Data are included for Boulder, Colorado for several dates in January, February and March, 1964. Six of these Umkehr evaluations were chosen for comparison with other methods of determining vertical ozone distributions.

The results of Umkehr evaluations are empirically corrected for cloudy conditions, hence the vertical distributions which are derived for cloudy conditions are presumably poorer, on the average, than those for clear sky conditions. It must be noted that the inverse method assumes no clouds. The effect of clouds, although certain to affect adversely the inversion results, has not been evaluated. Dütsch and Mateer (1964) classify cloudiness conditions with an index which varies from zero through five. Zero refers to a clear sky condition and five to a considerable cloud effect. The data chosen for comparison were taken during either clear or slightly cloudy conditions (i.e. an index of either zero or one) with the exception of the data for February 20, 1964, for which an index of three was assigned.

The results of the Umkehr evaluations are also presented in Figs. 6.1 through 6.6. Block distributions have been presented here although smooth curves could have been presented by using some technique for curve fitting through the midpoint values of each block. The position of the primary maximum is good in all figures, although the Umkehr blocks are somewhat broad in this region. The Umkehr distribution underestimates the ozone amount in the region of the primary maximum in all six figures. This ozone deficiency is generally compensated for by an overestimate at the top and bottom of the distributions. This is the same systematic

effect noted by Craig (1967). There appears to be an indication of the effects of the lower secondary maximum in the Umkehr data. The main peak is broadened at the bottom which tends to indicate an averaging which includes this secondary feature. This broadening is more prevalent in Figs. 6.3 through 6.6, which also coincides with the actual distributions with the most dominant secondary humps.

Comparison of Methods.

In the following discussion, the inversion method that is presented in this dissertation will be compared with other methods of determining vertical ozone distributions with the following considerations. Although the assumption of a plane-parallel atmosphere is unrealistic for practical studies, the technique which has been presented will have application if spherical effects can be included in the theory. This problem is unsolved as yet, however, the general inversion technique considered here may be applied to this problem when such a solution is found. In this case the results should be comparable to those presented with the plane-parallel assumption. With these comments in mind, the inversion method will be compared with other methods with the understanding that spherical effects must be included for practical validity.

The original ozonesonde data are considered to represent the actual ozone distributions, and therefore the other methods are compared with this only in the sense that it is an optimum result. Actually the ozonesonde data stop in the vicinity of 10 mb, above which a constant mixing ratio is assumed to exist. For this reason, the inversion method presented here (henceforth called the inverse method) and the Umkehr method are potentially better sounding techniques in the regions of the atmosphere above 10 mb. The former method is particularly effective at the top of the atmosphere. Since the Umkehr method has apparent systematic error effects and the statistical method indicates only average values, the inverse method seems to offer more promise for determining the ozone distribution above the 10 mb region.

Although the position of the main peak is fairly well defined by each method, the shape of the main peak is described most accurately by the statistical and inverse methods. Again the statistical method suffers because it is influenced to a large extent by the average distribution. This is evident in Figs. 6.4 and 6.5 where the actual distributions show deviations from the average values. Therefore, the inverse method is the better method for this region also. When errors are encountered in the experimental data, the ability to distinguish secondary features is lost for both the Umkehr and the inverse methods. The statistical

method often gives indications of typical seasonal features for a certain geographic location, but for any particular day little weight should be attached to these features. There is also little to choose from in the lower regions of the ozone distribution since, at best, each method can give only average or typical values.

As previously indicated, the total ozone content in a vertical column of the atmosphere is assumed independently known in the present problem. Both the Umkehr and inverse methods implicitly use the total ozone amount in calculating the vertical distribution. The results of both methods are consistent with the known total ozone contents and there is little difference on this basis.

CHAPTER VII

CONCLUSIONS AND SUGGESTED FUTURE RESEARCH

In the preceding chapters Twomey's inversion technique has been applied to the inversion of the radiative transfer equation in order to infer the vertical ozone distribution. This technique has only been applied for the case where the atmosphere is assumed to be plane-parallel. Results indicate that spherical effects must be included if this method is to have practical application. When spherical effects can be considered this inversion method shows promise for determining the vertical ozone distribution on a global surveillance basis where the detection system would be mounted on a satellite. This inversion method appears to be particularly promising for detecting the upper level ozone distribution and also in resolving the shape and position of the primary maximum. This method shows no particular bias toward some standard distribution, as opposed to other methods, such as the Umkehr method (see Mateer 1964) and the statistical method.

The time involved in reducing the data presents no apparent problem as the current computational time on the CDC 6600 computer at the NCAR facility in Boulder, Colorado is about two minutes. If such an indirect sounding method would be adopted, it would be advisable to use the standard

balloon-borne ozonesonde as a periodic check. Further, the total ozone amount should also be periodically monitored.

Future Research.

Several obvious studies are recommended for future research. The solution of the equation of radiative transfer where a spherical atmosphere is considered is needed in this problem and in many other atmospheric problems (i.e. twilight studies, total ozone determinations, etc.). A possible alternative to requiring the solution to the spherical problem involves reformulating the inverse problem to replace the variation in observing angle with a variation in wavelength. In this case one would observe the polarized intensity components emergent from the top of the atmosphere in the nadir as a function of wavelength. Under these circumstances curvature effects would be minimized.

Since all of the methods for determining the vertical ozone distribution considered in this dissertation assume that the total amount of ozone is independently known, one can easily understand the importance of accurately determining this parameter. Although there have been methods proposed for determining the value of this parameter from a satellite (Singer and Wentworth 1957, Dave and Mateer 1967) more work must be done in this area.

The effect of atmospheric aerosols is unknown. If these should prove to be a significant source of error in the wavelength regions of interest, one will be faced with

a major problem. In order to correct for absorption and scattering due to aerosols, one would very probably need to know the vertical number, size and type distribution as a function of geographic location and time. The problem of monitoring aerosols has proved to be extremely difficult.

The effect of cloud layers has been ignored. Not only are the scattering properties of various types of clouds poorly understood but, in addition, one would have to monitor the elevation and horizontal extent of the cloud layers.

The effect of ground reflectivity on the ozone inversion problem can be more readily determined once the character of the ultraviolet reflection at the ground has been determined. Some progress can be made without experimental data, however, by choosing various reflection models at the surface.

APPENDIX 1

The terminology and representations used in the description of the vertical distribution of ozone have been described in considerable detail by Godson (1962). The total amount of ozone in an atmospheric layer is commonly expressed in terms of its reduced thickness. This is the thickness, of a column of unit cross-section of pure ozone, which would result if all of the ozone in a vertical column of the atmospheric layer of interest were reduced to standard temperature (0°C) and pressure (1013.250 mb). To indicate that this is not a length unit, the column of ozone at STP is referred to in terms of atmosphere-centimeter units (atm-cm) or milli atmosphere-centimeters (m atm-cm). If all of the ozone in an atmospheric column, extending from the surface of the earth to the top of the atmosphere, were collected into a column at STP, the height of the column would be between two and six mm thick. Consequently, total ozone amounts are between 200 and 600 m atm-cm.

A common format for displaying vertical ozone distributions has been prepared by Godson (1962) and is known as an ozonagram. In this diagram the abscissa is

ozone partial pressure in μmb and the ordinate is the logarithm of atmospheric pressure in millibars (mb). Along the right hand side of the diagram is a height scale (km) corresponding to the pressure - height relationship in the standard atmosphere. The curved lines which slope from the upper left to the lower right in the diagram are lines of constant ozone mixing ratio in μg/g.

APPENDIX 2

The single scattering albedo for a particular atmospheric layer is defined as the ratio of the scattering optical depth for the layer, τ^s, to the total optical depth, τ, for that layer (i.e. $\tau=\tau^s+\tau^a$, where τ^a is the optical depth due to absorption for that layer). Hence the single scattering albedo may be written as

$$\omega = \frac{\tau^s}{\tau^s+\tau^a}. \qquad \text{(A-2.1)}$$

For numerical integrations over optical depth it is necessary to break the atmosphere into layers where the physical properties within each layer are approximately uniform. It is often convenient to describe mathematically the intensity of scattered light at specific levels for some problems and at midpoints of layers for others. The following example is worked out for the three layer model shown in Fig. A-2.1. This will demonstrate the relationship between the two descriptions. Each layer in Fig. A-2.1 represents an equal optical depth increment, $\Delta\tau$. The scattering optical depth for each layer is

$$\Delta\tau^s = \frac{K_\nu^s \Delta p}{g}, \qquad \text{(A-2.2)}$$

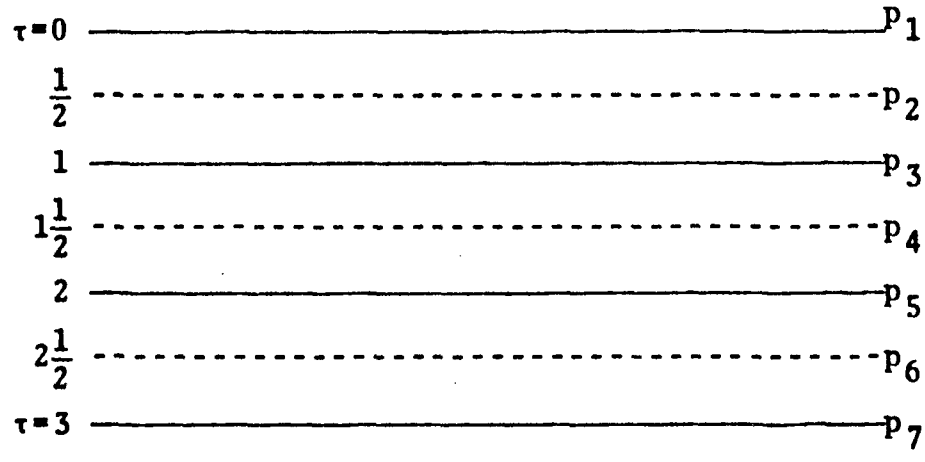

Fig. A-2.1. Three layer model atmosphere.

where K_ν^s is the appropriate mass scattering coefficient for the frequency ν, g is the gravitational constant and Δp is the pressure increment corresponding to the layer of interest. The subscript ν is omitted in the following equations.

The single scattering albedos which are defined at the levels (i.e. layers 1 and 2 in the example) are defined in terms of the properties over two layers, while the midpoint single scattering albedos are defined in terms of a single layer. The relationship should be apparent from the following calculations.

$$\omega(\tfrac{1}{2}) = \frac{K^s}{g}\frac{(p_3-p_1)}{\Delta\tau}$$

$$\omega(1) = \frac{K^s}{g}\frac{(p_5-p_1)}{2\Delta\tau} = \frac{K^s}{g}\frac{(p_5-p_3+p_3-p_1)}{2\Delta\tau} = \frac{\omega(1\frac{1}{2})+\omega(\frac{1}{2})}{2}$$

$$\omega(1\tfrac{1}{2}) = \frac{K^s}{g}\frac{(p_5-p_3)}{\Delta\tau}$$

$$\omega(2) = \frac{K^s}{g}\frac{(p_7-p_3)}{2\Delta\tau} = \frac{K^s}{g}\frac{(p_7-p_5+p_5-p_3)}{2\Delta\tau} = \frac{\omega(2\frac{1}{2})+\omega(1\frac{1}{2})}{2}$$

$$\omega(2\tfrac{1}{2}) = \frac{K^s}{g}\frac{(p_7-p_5)}{\Delta\tau}$$

It is often necessary to describe the vertical ozone distribution by both a pressure-partial pressure of ozone distribution (e.g. Fig. 5.4) and also a single scattering albedo - optical depth representation (e.g. Fig. 5.6). The partial pressure of ozone may be most conveniently related to atmospheric pressure by an ozonagram (e.g. Fig. 5.4). The equation that describes this relationship is

$$\bar{p}_3 \ (\mu\text{mb}) = \frac{0.55\Delta\Omega \ (\text{m atm-cm})}{\log_{10}(\frac{p_1}{p_2})} , \qquad \text{(A-2.3)}$$

where $\bar{p}_3$ is the average ozone partial pressure throughout the pressure increment $\Delta p = p_1 - p_2$ and $\Delta\Omega$ is the total ozone amount in this interval. The single scattering albedo may be related to the optical depth for this same interval since

$$\omega = \frac{\Delta\tau^s}{\Delta\tau} = \frac{\frac{K^s}{g}(p_1 - p_2)}{\frac{K^s}{g}(p_1 - p_2) + \alpha\Delta\Omega} . \qquad \text{(A-2.4)}$$

Frequently the optical depth increment is a constant for the problem. The Δp intervals are then selected, on the basis of the known ozone distribution and Eq. (A-2.4), to be consistent with this requirement. If, however, one is given the values of the single scattering albedo and the optical depth increment, one can calculate the corresponding pressure and total ozone increments in terms of

these quantities by manipulating Eq. (A-2.4) to get

$$\Delta p = \frac{g}{K^s}\omega\Delta\tau \qquad \text{(A-2.5)}$$

and

$$\Delta\Omega = \frac{\Delta\tau(1-\omega)}{\alpha} \; . \qquad \text{(A-2.6)}$$

APPENDIX 3

In this appendix a method will be described that allows one to predict a vertical ozone distribution on the basis of past records of ozone distributions and certain daily predictors. The following treatment is based on work done by Sellers (1957). This method reduces a series of correlated parameters to a smaller number of uncorrelated parameters. Here the correlated parameters are standardized ozone partial pressures at different atmospheric levels. A standardized partial pressure is defined to be the ozone partial pressure anomaly divided by the standard deviation of this ozone partial pressure at a particular atmospheric pressure level. Evenly spaced points are not required in the following development.

Let (P) be an nxm matrix of standardized ozone partial pressures at m selected pressure levels over a specific geographical location for a series of n days. These correlated parameters, the elements of the matrix (P), may be related to an uncorrelated orthogonal set, the elements of the matrix (R), by a rotation of coordinates described by

$$(P)=(R)(S), \qquad \text{(A-3.1)}$$

where (S) is also an orthogonal matrix. One can further require that (S) be orthonormal with no loss in generality. The matrix (R) will be more explicitly discussed later and

for the present will be considered to be the matrix satisfying Eq. (A-3.1).

The symmetric matrix (T) may now be formed by performing the following matrix operations.

$$(T)=(P)^*(P)=(S)^*(R)^*(R)(S) \qquad \text{(A-3.2)}$$

Here $(P)^*$, $(S)^*$ and $(R)^*$ are the corresponding transposed matrices of (P), (S) and (R). Since (T) is symmetric, one can select the orthonormal matrix (S) so that the product $(S)(T)(S)^*$ is a diagonal matrix (G) (Cramer 1946). That is,

$$(S)(T)(S)^*=(S)(S)^*(R)^*(R)(S)(S)^*=(R)^*(R)=(G), \qquad \text{(A-3.3)}$$

which also shows that the columns of the matrix (R) are orthogonal (i.e. uncorrelated). Now using the orthonormal properties of (S) one can form

$$(S)^*(S)(T)(S)^*=(T)(S)^*=(S)^*(G). \qquad \text{(A-3.4)}$$

Eq. (A-3.4) is an eigenvalue equation, where the column vectors of the square matrix $(S)^*$ are the eigenvectors. The eigenvalue that corresponds to the Kth column of $(S)^*$ is the element g_{KK} of the matrix (G). The solution to Eq. (A-3.4) may be performed by standard library subroutines available in most computer facility libraries. Once the eigenvectors (i.e. the columns of the matrix $(S)^*$) are known, the matrix (R) may be determined, using Eq. (A-3.1) and the orthonormal properties of the matrix (S), from

$$(R)=(P)(S)^*. \qquad \text{(A-3.5)}$$

Table A-3.1

Predictors Used in the Statistical Method.

Solar Indices (For lag periods of -3 to +10 days)

1. Sum of Fredericksburg 3-hr range indices
2. Average Amplitudes
3. Magnetic Character Figures C_p
4. Sunspot number
5. Magnetic Character Figures C_i
6. Solar Flare Index

Lunar Data

1. Number of days past either new or full moon
2. Number of days past full moon

Terrestrial Data

1. Temperatures at 15,20,50,100,200,300 and 700 mb
2. Surface pressure
3. Tropopause height
4. Total ozone

In the ozone problem, (S)=f(z) and (R)=f(t), where (S) could be compared to either spherical harmonics or to polynomials, in which case, (R) would be analogous to the time dependent amplitudes of the harmonics or polynomials.

The matrix (R) was calculated from 72 days of ozonesonde data for January and February during the three year period 1964, 1965 and 1966. These data, which consisted of ozone partial pressures at standard pressure levels, were obtained for Boulder, Colorado and were published by Dütsch (1966). The eleven days in 1964, which included the six days presented in this paper that corresponded to days of Umkehr evaluations at Boulder, were omitted from the record.

Each set of the amplitude functions, the elements of the matrix (R), was correlated with various solar, lunar and terrestrial quantities to determine the feasibility of predicting these functions. The various predictors considered are listed in Table A-3.1. The only predictor that explained more than 4% of the total variance was the total ozone, which accounted for about 78% of the variance of the second eigenvector and about 16% of the total variance. The total ozone was used to predict the elements of the matrix (R) which is then used with the matrix (S) in Eq. (A-3.1) to calculate the ozone partial pressures at the standard height levels. Because the only significant amount of explained

variance is associated with the second eigenvector, the only nonzero row in the matrix (S) is the second row. The resulting matrix (P) was normalized to give the observed total ozone amount.

REFERENCES

Atmospheric Ozone Studies, 1966: Publication 1348, Washington D. C., National Academy of Sciences, National Research Council, 21 pp.

Bandeen, W. R., 1966: Radiation Physics. Satellite Data in Meteorological Research. NCAR Tech Notes, NCAR-TN-11, 229-249.

Bôcher, M., 1922: Introduction to Higher Algebra. New York, The Macmillan Co., 43-52.

Brewer, A. W., and J. R. Milford, 1960: The Oxford-Kew Ozone Sonde. Proc. Phys. Soc. London, A256, 470-495.

Craig, R. A., 1948: The Observations and Photochemistry of Atmospheric Ozone and Their Meteorological Significance. D. Sc. Thesis, Mass. Inst. Tech.

Craig, R. A., J. J. DeLuisi and I. Stuetzer, 1967: Comparison of Chemiluminescent and Umkehr Observations of Ozone. J. Geophys. Res., 72, 1667-1671.

Cramers, H. C., 1946: Mathematical Methods of Statistics. Princeton, Princeton Univ. Press, 575 pp. See Chap 11.

Dave, J. V., 1964: Meaning of successive iteration of the auxiliary equation in the theory of radiative transfer. Astrophys. J., 140, 1292-1303.

Dave, J. V., P. A. Sheppard and L. D. Walshaw, 1962: The vertical distribution of atmospheric ozone by methods of infra-red spectroscopy and related problem of the atmospheric continuum. Tech. Rep. Contract No. AF 6110521-84, Meteorology Department, Imperial College, London, S. W. 7, England, 78 pp.

Dave, J. V. and W. H. Walker, 1966: Convergence of the iterative solution of the auxiliary equations for Rayleigh scattering. Astrophys. J., 144, 798-808.

Dave, J. V. and C. L. Mateer, 1967: A preliminary study on the possibility of estimating total atmospheric ozone from satellite measurements. This paper has been accepted for publication in J. Atmos. Sci.

Dütsch, H. U., 1946: Photochemische Theorie des Atmospharischen Ozons unter Beriicksichtigung von Nichtgleichgewichtszustanden und Luftbewegungen. Doctoral dissertation, University of Zurich.

Dütsch, H. U., 1966: Two years of regular ozone soundings over Boulder, Colorado. NCAR Tech. Notes. NCAR-TN-10, 443 pp.

Dütsch, H. U. and L. L. Mateer, 1964: Uniform evaluation of Umkehr observations from the world ozone network. Part II. The vertical distribution of ozone. Boulder, National Center for Atmospheric Research, 202 pp.

Epstein, E. S., C. Osterberg, and A. Adel, 1956: A new method for the determination of the vertical distribution of ozone from a ground station. J. Met., 13, 319-334.

Fleming, H. E. and D. Q. Wark, 1965: A numerical method for determining the relative spectral response of the vidicone in a Nimbus satellite system. Applied Optics., 4, 337-342.

Godson, W. L., 1962: The representation and analysis of vertical distributions of ozone. Quart. J. Roy. Met. Soc., 88, 220-232.

Goody, R. M., and W. T. Roach, 1956: Determination of the vertical distribution of ozone from emission spectra. Quart J. Roy. Met. Soc., 82, 217-221.

Gotz, F. W. P., 1931: Zum Stiahlungsklima des Spitzbergen Sommers. Gerlands Beitrage zur Geophys., 31, 119-154.

Hamming, R. W., 1962: Numerical Methods for Scientists and Engineers. New York, McGraw-Hill Book Company, Inc., 441 pp.

Hering, W. S., 1964: Ozonesonde observations over North America, Volume 1. AFCRL-64-30 (1).

Hering, W. S. and T. R. Borden, Jr., 1964: Ozonesonde observations over North America, Volume 2. AFCRL-64-30(11).

Hering, W. S., and T. R. Borden, Jr., 1965: Ozonesonde observations over North America Volume 3. AFCRL-64-30(111).

Herman, B. M., 1963: A Numerical Solution to the Equation of Radiative Transfer for Particles in the Mie Region. Ph.D. dissertation, University of Arizona.

Herman, B. M., and S. R. Browning, 1965: A numerical solution to the equation of radiative transfer. J. Atmos. Sci. 22, 559-566.

Herman, B. M., and D. N. Yarger, 1965: The effect of absorption on a Rayleigh atmosphere. J. Atmos. Sci. 22, 644-651.

Kaplan, L. D., 1961: The spectroscope as a tool for atmospheric sounding by satellites. J. Quant. Spectrosc. Radiat. Transfer, 1, 89-95.

King, J. I. F., 1966: Radiation Physics. Satellite Data in Meteorological Research. NCAR Tech. Notes, NCAR-TN-11, 261-278.

Kulcke, W., and H. K. Paetzold, 1957: Uber un Radiosonde zur Bestimmung der vertikalen Ozonverteilung. Ann. d. Met., 8, 47-53.

Margenau, H. and G. W. Murphy, 1956: The Mathematics of Physics and Chemistry. Princeton, N. J., D. Van Nostrand Company, Inc., 604 pp.

Mateer, C. L., 1964: A study of the information content of Umkehr observations. Tech. Rep. No. 2, Project 04682. Department of Meteorology and Oceanography, The University of Michigan, Ann Arbor. 199 pp.

Mateer, C. L., and H. U. Dütsch, 1964: Uniform evaluation of Umkehr observations from the world ozone network. Part 1. Proposed standard Umkehr evaluation technique. Boulder, National Center for Atmospheric Research, 105 pp.

Miller, D. E,, and K. H. Stewart, 1965: Observations of atmospheric ozone from an artificial earth satellite. Proc. Roy. Soc. London, A288, 540-544.

Möller, F., 1961: Atmospheric Water vapor Measurements at 6-7 microns from a satellite. Planet. Space Sci., 5, 202-206.

Möller, F., 1962: Einige Vorlaufige Auswertungen der Strahlungsmessungen von Tiros II. Arch. Meteorol. Geophys. Bioklimatol. Ser B., 12 (1), 78-94.

Möller, F. and E. Raschke, 1964: Evaluation of Tiros III radiation data. Contractor Report CR-112, National Aeronautics and Space Administration, Washington, D. C.

Newkirk, G. Jr. and J. A. Eddy, 1964: Light scattering by particles in the upper atmosphere. J. Atmos. Sci, 21, 35-60.

Phillips, B. L., 1962: A technique for the numerical solution of certain integral equations of the first kind. Journ. Assoc. Comp. Mach., 9, 84-97.

Pittock, A. B., 1963: Determination of the vertical distribution of ozone by twilight balloon photometry. J. Geophys. Res., 68, 5143-5155.

Rados, R. M., 1967: The evolution of the TIROS meteorological satellite operational system. Bull. Am. Meteor. Soc. 48, 326-337.

Ramanathan, K. R., and J. V. Dave, 1957: The calculation of the vertical distribution of ozone by the Gotz Umkehr-effect (Method B). Ann I. G. Y., 5 (1), 23-45.

Rawcliffe, R. D., G. E. Meloy, R. M. Friedman, and E. H. Rogers, 1963: Measurement of vertical distribution of ozone from a polar orbiting satellite. J. Geophys. Res., 68, 6425-6429.

Regener, E., and V. H. Regener, 1934: Aufnahme des ultravioletten Sonnenspektrums in der Stratosphare und die verticale Ozonverteiheng. Phys. Zeit., 35, 788-793.

Regener, V. H., 1960: On a sensitive method for the recording of atmospheric ozone. J. Geophys. Res., 65, 3975-3977.

Schröer, E., 1949: Theorie der Entstehung, Zersetzung, und Vertailung des atmospharischen Ozons. Berichte des Deutschen Wetterdienstes in der U. S. Zone, No. 11, 13-23.

Sekera, Z., 1963: Radiative transfer in a planetary atmosphere with imperfect scattering. Rept. No. R-143-PR, Contract AF 49(638)-700, Rand Corporation, 64 pp.

Sekera, Z., 1966: Inverion methods. Satellite Data in Meteorological Research. NCAR Tech. Notes, NCAR-TN-11, 299-310.

Sekera, Z., and J. V. Dave, 1961: Determination of the vertical distribution of ozone from the measurement of diffusely reflected ultra-violet solar-radiation. Planet. Space Sci., 5, 122-136.

Sellers, W. D., 1957: A statistical-dynamic approach to numerical weather prediction. Sci. Rept. No. 2, Dept. of Met., M.I.T., 151 pp.

Singer, S. F. and R. C. Wentworth, 1957: A method for the determination of the vertical ozone distribution from a satellite. J. Geophys. Res., 62, 299-308.

Sokolnikoff, I. S., 1956: Mathematical Theory of Elasticity. New York, McGraw-Hill Book Company, Inc., 476 pp.

Stokes, G. G., 1852: Trans. Cont. Phil. Soc., 9, 399 pp.

Twomey, S., 1961: On the deduction of the vertical distribution of ozone by ultraviolet spectral measurements from a satellite. J. Geophys. Res., 66, 2153-2162.

Twomey, S., 1963: On the numerical solution of Fredholm integral equations of the first kind by the inversion of the linear system produced by quadrature. Jour. Asso. Comp. Mach., 10, 97-101.

Twomey, S., 1965: The application of numerical filtering to the solution of integral equations encountered in indirect sensing measurements. Jour. Franklin Inst., 279, 95-109.

Twomey, S., and H. B. Howell, 1963: A discussion of indirect sounding methods with special reference to the deduction of vertical ozone distribution from light scattering measurements. Mon. Wea. Rev., 91, 659-664.

Vassey, A., 1958: Radio-sonde speciale pour da mesure de la repartition verticale de l'ozone atmospherique. J. Sci. Met., 10, 63-75.

Venkateswaran, S. V., J.G. Moore, and A. J. Kreuger, 1961: Determination of the vertical distribution of ozone by satellite photometry. J. Geophys. Res., 66, 1751-1771.

Wangsness, R. K., 1963: Introductory Topics in Theoretical Physics: Relativity, Thermodynamics, Kinetic Theory, and Statistical Mechanics. New York, John Wiley and Sons, Inc. 315 pp.

Wark, D. Q. and H. E. Fleming, 1966: Indirect Measurements of atmospheric temperature profiles from satellites: 1. Introduction. Mon. Weather Rev., 94, 351-362.

Willett, H. C., 1965: Climatic evidence on probable physical nature of solar disturbance of climatic patterns. NCAR Tech. Notes, NCAR-TN-8, 175-188.